

Chapter 3

The Standard Model of Electroweak Interactions



Guido Altarelli and Stefano Forte

3.1 Introduction

In this chapter,¹ we summarize the structure of the standard EW theory [1] and specify the couplings of the intermediate vector bosons W^\pm , Z and of the Higgs particle with the fermions and among themselves, as dictated by the gauge symmetry plus the observed matter content and the requirement of renormalizability. We discuss the realization of spontaneous symmetry breaking and of the Higgs mechanism [2]. We then review the phenomenological implications of the EW theory for collider physics (that is we leave aside the classic low energy processes that are well described by the “old” weak interaction theory (see, for example, [3])). Moreover, a detailed description of experiments for precision tests of the EW theory is presented in Chap. 6.

For this discussion we split the lagrangian into two parts by separating the terms with the Higgs field:

$$\mathcal{L} = \mathcal{L}_{\text{gauge}} + \mathcal{L}_{\text{Higgs}} . \tag{3.1}$$

Both terms are written down as prescribed by the $SU(2) \otimes U(1)$ gauge symmetry and renormalizability, but the Higgs vacuum expectation value (VEV) induces the

The author “G. Altarelli” is deceased at the time of publication.

¹See Chap. 2 for a general introduction to Chap. 2–4 with updated references.

G. Altarelli
University of Rome 3, Rome, Italy

S. Forte (✉)
Dipartimento di Fisica, Università di Milano, Milano, Italy

spontaneous symmetry breaking responsible for the non vanishing vector boson and fermion masses.

3.2 The Gauge Sector

We start by specifying $\mathcal{L}_{\text{gauge}}$, which involves only gauge bosons and fermions, according to the general formalism of gauge theories discussed in Chap. 2:

$$\mathcal{L}_{\text{gauge}} = -\frac{1}{4} \sum_{A=1}^3 F_{\mu\nu}^A F^{A\mu\nu} - \frac{1}{4} B_{\mu\nu} B^{\mu\nu} + \bar{\psi}_L i \gamma^\mu D_\mu \psi_L + \bar{\psi}_R i \gamma^\mu D_\mu \psi_R. \quad (3.2)$$

This is the Yang–Mills lagrangian for the gauge group $SU(2) \otimes U(1)$ with fermion matter fields. Here

$$B_{\mu\nu} = \partial_\mu B_\nu - \partial_\nu B_\mu \quad \text{and} \quad F_{\mu\nu}^A = \partial_\mu W_\nu^A - \partial_\nu W_\mu^A - g \epsilon_{ABC} W_\mu^B W_\nu^C \quad (3.3)$$

are the gauge antisymmetric tensors constructed out of the gauge field B_μ associated with $U(1)$, and W_μ^A corresponding to the three $SU(2)$ generators; ϵ_{ABC} are the group structure constants (see Eqs. (3.8, 3.9)) which, for $SU(2)$, coincide with the totally antisymmetric Levi-Civita tensor (recall the familiar angular momentum commutators). The normalization of the $SU(2)$ gauge coupling g is therefore specified by Eq. (3.3).

The fermion fields are described through their left-hand and right-hand components:

$$\psi_{L,R} = [(1 \mp \gamma_5)/2] \psi, \quad \bar{\psi}_{L,R} = \bar{\psi} [(1 \pm \gamma_5)/2], \quad (3.4)$$

with γ_5 and other Dirac matrices defined as in the book by Bjorken–Drell [4]. In particular, $\gamma_5^2 = 1$, $\gamma_5^\dagger = \gamma_5$. Note that, as given in Eq. (3.4),

$$\bar{\psi}_L = \psi_L^\dagger \gamma_0 = \psi^\dagger [(1 - \gamma_5)/2] \gamma_0 = \bar{\psi} \gamma_0 [(1 - \gamma_5)/2] \gamma_0 = \bar{\psi} [(1 + \gamma_5)/2].$$

The matrices $P_\pm = (1 \pm \gamma_5)/2$ are projectors. They satisfy the relations $P_\pm P_\pm = P_\pm$, $P_\pm P_\mp = 0$, $P_+ + P_- = 1$.

The sixteen linearly independent Dirac matrices can be divided into γ_5 -even and γ_5 -odd according to whether they commute or anticommute with γ_5 . For the γ_5 -even, we have

$$\bar{\psi} \Gamma_E \psi = \bar{\psi}_L \Gamma_E \psi_R + \bar{\psi}_R \Gamma_E \psi_L \quad (\Gamma_E \equiv 1, i \gamma_5, \sigma_{\mu\nu}), \quad (3.5)$$

whilst for the γ_5 -odd,

$$\bar{\psi}\Gamma_O\psi = \bar{\psi}_L\Gamma_O\psi_L + \bar{\psi}_R\Gamma_O\psi_R \quad (\Gamma_O \equiv \gamma_\mu, \gamma_\mu\gamma_5). \quad (3.6)$$

The standard EW theory is a chiral theory, in the sense that ψ_L and ψ_R behave differently under the gauge group (so that parity and charge conjugation non conservation are made possible in principle). Thus, mass terms for fermions (of the form $\bar{\psi}_L\psi_R + \text{h.c.}$) are forbidden in the symmetric limit. In particular, in the Minimal Standard Model (MSM: i.e. the model that only includes all observed particles plus a single Higgs doublet), all ψ_L are $SU(2)$ doublets while all ψ_R are singlets. But for the moment, by $\psi_{L,R}$ we mean column vectors, including all fermion types in the theory that span generic reducible representations of $SU(2) \otimes U(1)$.

In the absence of mass terms, there are only vector and axial vector interactions in the lagrangian and those have the property of not mixing ψ_L and ψ_R . Fermion masses will be introduced, together with W^\pm and Z masses, by the mechanism of symmetry breaking. The covariant derivatives $D_\mu\psi_{L,R}$ are explicitly given by

$$D_\mu\psi_{L,R} = \left[\partial_\mu + ig \sum_{A=1}^3 t_{L,R}^A W_\mu^A + ig' \frac{1}{2} Y_{L,R} B_\mu \right] \psi_{L,R}, \quad (3.7)$$

where $t_{L,R}^A$ and $1/2Y_{L,R}$ are the $SU(2)$ and $U(1)$ generators, respectively, in the reducible representations $\psi_{L,R}$. The commutation relations of the $SU(2)$ generators are given by

$$[t_L^A, t_L^B] = i \epsilon_{ABC} t_L^C \quad \text{and} \quad [t_R^A, t_R^B] = i \epsilon_{ABC} t_R^C. \quad (3.8)$$

We use the normalization (3.8) [in the fundamental representation of $SU(2)$]. The electric charge generator Q (in units of e , the positron charge) is given by

$$Q = t_L^3 + 1/2 Y_L = t_R^3 + 1/2 Y_R. \quad (3.9)$$

Note that the normalization of the $U(1)$ gauge coupling g' in (3.7) is now specified as a consequence of (3.9). Note that $t_R^i\psi_R = 0$, given that, for all known quark and leptons, ψ_R is a singlet. But in the following, we keep $t_R^i\psi_R$ for generality, in case 1 day a non singlet right-handed fermion is discovered.

3.3 Couplings of Gauge Bosons to Fermions

All fermion couplings of the gauge bosons can be derived directly from Eqs. (3.2) and (3.7). The charged W_μ fields are described by $W_\mu^{1,2}$, while the photon A_μ and weak neutral gauge boson Z_μ are obtained from combinations of W_μ^3 and B_μ . The

charged-current (CC) couplings are the simplest. One starts from the $W_\mu^{1,2}$ terms in Eqs. (3.2) and (3.7) which can be written as:

$$\begin{aligned} g(t^1 W_\mu^1 + t^2 W_\mu^2) &= g \left\{ [(t^1 + i t^2)/\sqrt{2}](W_\mu^1 - i W_\mu^2)/\sqrt{2} + \text{h.c.} \right\} \\ &= g \left\{ [(t^+ W_\mu^-)/\sqrt{2}] + \text{h.c.} \right\} , \end{aligned} \quad (3.10)$$

where $t^\pm = t^1 \pm i t^2$ and $W^\pm = (W^1 \pm i W^2)/\sqrt{2}$. By applying this generic relation to L and R fermions separately, we obtain the vertex

$$V_{\bar{\psi}\psi W} = g \bar{\psi} \gamma_\mu \left[(t_L^+/\sqrt{2})(1 - \gamma_5)/2 + (t_R^+/\sqrt{2})(1 + \gamma_5)/2 \right] \psi W_\mu^- + \text{h.c.} \quad (3.11)$$

Given that $t_R = 0$ for all fermions in the SM, the charged current is pure $V - A$. In the neutral-current (NC) sector, the photon A_μ and the mediator Z_μ of the weak NC are orthogonal and normalized linear combinations of B_μ and W_μ^3 :

$$\begin{aligned} A_\mu &= \cos \theta_W B_\mu + \sin \theta_W W_\mu^3 , \\ Z_\mu &= -\sin \theta_W B_\mu + \cos \theta_W W_\mu^3 . \end{aligned} \quad (3.12)$$

and conversely:

$$\begin{aligned} W_\mu^3 &= \sin \theta_W A_\mu + \cos \theta_W Z_\mu , \\ B_\mu &= \cos \theta_W A_\mu - \sin \theta_W Z_\mu . \end{aligned} \quad (3.13)$$

Equations (3.12) define the weak mixing angle θ_W . We can rewrite the W_μ^3 and B_μ terms in Eqs. (3.2) and (3.7) as follows:

$$\begin{aligned} g t^3 W_\mu^3 + g' Y/2 B_\mu &= [g t^3 \sin \theta_W + g'(Q - t^3) \cos \theta_W] A_\mu + \\ &+ [g t^3 \cos \theta_W - g'(Q - t^3) \sin \theta_W] Z_\mu , \end{aligned} \quad (3.14)$$

where Eq. (3.9) for the charge matrix Q was also used. The photon is characterized by equal couplings to left and right fermions with a strength equal to the electric charge. Thus we immediately obtain

$$g \sin \theta_W = g' \cos \theta_W = e , \quad (3.15)$$

or equivalently,

$$\text{tg } \theta_W = g'/g \quad (3.16)$$

Once θ_W has been fixed by the photon couplings, it is a simple matter of algebra to derive the Z couplings, with the result

$$V_{\bar{\psi}\psi Z} = \frac{g}{2 \cos \theta_W} \bar{\psi} \gamma_\mu [t_L^3(1 - \gamma_5) + t_R^3(1 + \gamma_5) - 2Q \sin^2 \theta_W] \psi Z^\mu, \quad (3.17)$$

where $V_{\bar{\psi}\psi Z}$ is a notation for the vertex. Once again, recall that in the MSM, $t_R^3 = 0$ and $t_L^3 = \pm 1/2$.

In order to derive the effective four-fermion interactions that are equivalent, at low energies, to the CC and NC couplings given in Eqs. (3.11) and (3.17), we anticipate that large masses, as experimentally observed, are provided for W^\pm and Z by $\mathcal{L}_{\text{Higgs}}$. For left–left CC couplings, when the momentum transfer squared can be neglected, with respect to m_W^2 , in the propagator of Born diagrams with single W exchange (see, for example, the diagram for μ decay in Fig. 3.1, from Eq. (3.11)) we can write

$$\mathcal{L}_{\text{eff}}^{\text{CC}} \simeq \frac{g^2}{8m_W^2} [\bar{\psi} \gamma_\mu (1 - \gamma_5) t_L^+ \psi] [\bar{\psi} \gamma^\mu (1 - \gamma_5) t_L^- \psi]. \quad (3.18)$$

By specializing further in the case of doublet fields such as $\nu_e - e^-$ or $\nu_\mu - \mu^-$, we obtain the tree-level relation of g with the Fermi coupling constant G_F precisely measured from μ decay (see Chap. 2, Eqs. (2), (3)):

$$G_F / \sqrt{2} = g^2 / 8m_W^2. \quad (3.19)$$

By recalling that $g \sin \theta_W = e$, we can also cast this relation in the form

$$m_W = \mu_{\text{Born}} / \sin \theta_W, \quad (3.20)$$

with

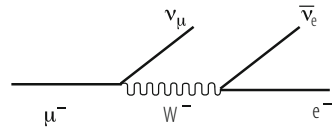
$$\mu_{\text{Born}} = (\pi \alpha / \sqrt{2} G_F)^{1/2} \simeq 37.2802 \text{ GeV}, \quad (3.21)$$

where α is the fine-structure constant of QED ($\alpha \equiv e^2 / 4\pi = 1/137.036$).

In the same way, for neutral currents we obtain in Born approximation from Eq. (3.17) the effective four-fermion interaction given by

$$\mathcal{L}_{\text{eff}}^{\text{NC}} \simeq \sqrt{2} G_F \rho_0 \bar{\psi} \gamma_\mu [\dots] \psi \bar{\psi} \gamma^\mu [\dots] \psi, \quad (3.22)$$

Fig. 3.1 The Born diagram for μ decay



where

$$[\dots] \equiv t_L^3(1 - \gamma_5) + t_R^3(1 + \gamma_5) - 2Q \sin^2 \theta_W \quad (3.23)$$

and

$$\rho_0 = \frac{m_W^2}{m_Z^2 \cos^2 \theta_W} . \quad (3.24)$$

All couplings given in this section are obtained at tree level and are modified in higher orders of perturbation theory. In particular, the relations between m_W and $\sin \theta_W$ (Eqs. (3.20) and (3.21)) and the observed values of ρ ($\rho = \rho_0$ at tree level) in different NC processes, are altered by computable EW radiative corrections, as discussed in Sect. (3.11).

The partial width $\Gamma(W \rightarrow \bar{f} f')$ is given in Born approximation by the simplest diagram in Fig. 3.2 and one readily obtains from Eq. (3.11) with $t_R = 0$, in the limit of neglecting the fermion masses and summing over all possible f' for a given f :

$$\Gamma(W \rightarrow \bar{f} f') = N_C \frac{G_F m_W^3}{6\pi\sqrt{2}} = N_C \frac{\alpha m_W}{12 \sin^2 \theta_W}, \quad (3.25)$$

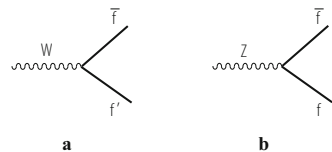
where $N_C = 3$ or 1 is the number of colours for quarks or leptons, respectively, and the relations Eqs. (3.15, 3.19) have been used. Here and in the following expressions for the Z widths the one loop QCD corrections for the quark channels can be absorbed in a redefinition of N_C : $N_C \rightarrow 3[1 + \alpha_s(m_Z)/\pi + \dots]$. Note that the widths are particularly large because the rate already occurs at order g^2 or G_F . The experimental values of the W total width and the leptonic branching ratio (the average of e , μ and τ modes) are [5, 8] (see Chap. 6):

$$\Gamma_W = 2.147 \pm 0.060 \text{ GeV}, \quad B(W \rightarrow l\nu_l) = 10.80 \pm 0.09. \quad (3.26)$$

The branching ratio B is in very good agreement with the simple approximate formula, derived from Eq. (3.25):

$$B(W \rightarrow l\nu_l) \sim \frac{1}{2 \cdot 3 \cdot (1 + \alpha_s(m_Z^2)/\pi) + 3} \sim 10.8\%. \quad (3.27)$$

Fig. 3.2 Diagrams for (a) the W and (b) the Z widths in Born approximation



The denominator corresponds to the sum of the final states $d'\bar{u}$, $s'\bar{c}$, $e^-\bar{\nu}_e$, $\mu^-\bar{\nu}_\mu$, $\tau^-\bar{\nu}_\tau$ (for the definition of d' and s' see Eq. (3.66)).

For $t_R = 0$ the Z coupling to fermions in Eq. (3.17) can be cast into the form:

$$V_{\bar{\psi}_f\psi_f Z} = \frac{g}{2 \cos \theta_W} \bar{\psi}_f \gamma_\mu [g_V^f - g_A^f \gamma_5] \psi_f Z^\mu, \quad (3.28)$$

with:

$$g_A^f = t_L^{3f}, \quad g_V^f/g_A^f = 1 - 4|Q_f| \sin^2 \theta_W. \quad (3.29)$$

and $t_L^{3f} = \pm 1/2$ for up-type or down-type fermions. In terms of $g_{A,V}$ given in Eqs. (3.29) (the widths are proportional to $(g_V^2 + g_A^2)$), the partial width $\Gamma(Z \rightarrow \bar{f}f)$ in Born approximation (see the diagram in Fig. 3.2), for negligible fermion masses, is given by:

$$\begin{aligned} \Gamma(Z \rightarrow \bar{f}f) &= N_C \frac{\alpha m_Z}{12 \sin^2 2\theta_W} [1 + (1 - 4|Q_f| \sin^2 \theta_W)^2] \\ &= N_C \rho_0 \frac{G_F m_Z^3}{24\pi \sqrt{2}} [1 + (1 - 4|Q_f| \sin^2 \theta_W)^2]. \end{aligned} \quad (3.30)$$

where $\rho_0 = m_W^2/m_Z^2 \cos^2 \theta_W$ is given in Eq. (3.55). The experimental values of the Z total width and of the partial rates into charged leptons (average of e , μ and τ), into hadrons and into invisible channels are [5, 8] (see Chap. 6):

$$\begin{aligned} \Gamma_Z &= 2.4952 \pm 0.0023 \text{ GeV}, \\ \Gamma_{l+l^-} &= 83.985 \pm 0.086 \text{ MeV}, \\ \Gamma_h &= 1744.4 \pm 2.0 \text{ MeV}, \\ \Gamma_{inv} &= 499.0 \pm 1.5 \text{ MeV}. \end{aligned} \quad (3.31)$$

The measured value of the Z invisible width, taking radiative corrections into account, leads to the determination of the number of light active neutrinos (see Chap. 6):

$$N_\nu = 2.9841 \pm 0.0083, \quad (3.32)$$

well compatible with the three known neutrinos ν_e , ν_μ and ν_τ ; hence there exist only the three known sequential generations of fermions (with light neutrinos), a result with important consequences also in astrophysics and cosmology.

At the Z peak, besides total cross sections, various types of asymmetries have been measured. The results of all asymmetry measurements are quoted in terms of the asymmetry parameter A_f , defined in terms of the effective coupling constants,

g_V^f and g_A^f , as:

$$A_f = 2 \frac{g_V^f g_A^f}{g_V^{f2} + g_A^{f2}} = 2 \frac{g_V^f / g_A^f}{1 + (g_V^f / g_A^f)^2}, \quad A_{FB}^f = \frac{3}{4} A_e A_f. \quad (3.33)$$

The measurements are: the forward-backward asymmetry ($A_{FB}^f = (3/4)A_e A_f$), the tau polarization (A_τ) and its forward backward asymmetry (A_e) measured at LEP, as well as the left-right and left-right forward-backward asymmetry measured at SLC (A_e and A_f , respectively). Hence the set of partial width and asymmetry results allows the extraction of the effective coupling constants: widths measure ($g_V^2 + g_A^2$) and asymmetries measure g_V/g_A .

The top quark is heavy enough that it can decay into a real bW pair, which is by far its dominant decay channel. The next mode, $t \rightarrow sW$, is suppressed in rate by a factor $|V_{ts}|^2 \sim 1.7 \cdot 10^{-3}$, see Eqs. (3.71–3.73). The associated width, neglecting m_b effects but including 1-loop QCD corrections in the limit $m_W = 0$, is given by (we have omitted a factor $|V_{tb}|^2$ that we set equal to 1):

$$\Gamma(t \rightarrow bW^+) = \frac{G_F m_t^3}{8\pi\sqrt{2}} \left(1 - \frac{m_W^2}{m_t^2}\right)^2 \left(1 + 2\frac{m_W^2}{m_t^2}\right) \left[1 - \frac{\alpha_s(m_Z)}{3\pi} \left(\frac{2\pi^2}{3} - \frac{5}{2}\right) + \dots\right]. \quad (3.34)$$

The top quark lifetime is so short, about $0.5 \cdot 10^{-24}$ s, that it decays before hadronizing or forming toponium bound states.

3.4 Gauge Boson Self-interactions

The gauge boson self-interactions can be derived from the $F_{\mu\nu}$ term in $\mathcal{L}_{\text{gauge}}$, by using Eq. (3.12) and $W^\pm = (W^1 \pm iW^2)/\sqrt{2}$.

Defining the three-gauge-boson vertex as in Fig. 3.3 (with all incoming lines), we obtain ($V \equiv \gamma, Z$)

$$V_{W^-W^+V} = ig_{W^-W^+V} [g_{\mu\nu}(p-q)_\lambda + g_{\mu\lambda}(r-p)_\nu + g_{\nu\lambda}(q-r)_\mu], \quad (3.35)$$

with

$$g_{W^-W^+\gamma} = g \sin\theta_W = e \quad \text{and} \quad g_{W^-W^+Z} = g \cos\theta_W. \quad (3.36)$$

Note that the photon coupling to the W is fixed by the electric charge, as imposed by QED gauge invariance. The ZWW coupling is larger by a $\tan\theta_W$ factor. This form of the triple gauge vertex is very special: in general, there could be departures from the above SM expression, even restricting us to Lorentz invariant, em gauge

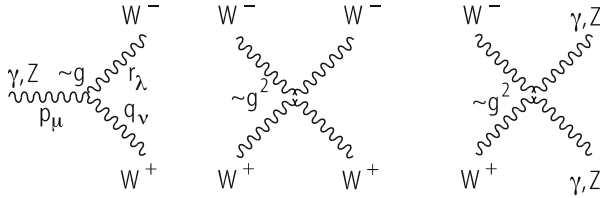


Fig. 3.3 The three- and four-gauge boson vertices. The cubic coupling is of order g , while the quartic one is of order g^2

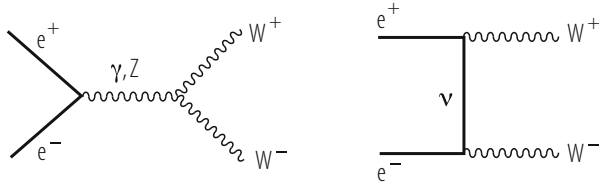


Fig. 3.4 The three- and four-gauge boson vertices. The cubic coupling is of order g , while the quartic one is of order g^2

symmetric and C and P conserving couplings. In fact some small corrections are already induced by the radiative corrections. But, in principle, more important could be the modifications induced by some new physics effect. The experimental testing of the triple gauge vertices has been done mainly at LEP2 and at the Tevatron. At LEP2 the crosssection and angular distributions for the process $e^+e^- \rightarrow W^+W^-$ have been studied (see Chap. 6).

In Born approximation the Feynman diagrams for the LEP2 process are shown in Fig. 3.4 [6]. Besides neutrino exchange which only involves the well established charged current vertex, the triple weak gauge vertices $V_{W^-W^+\nu}$ appear in the γ and Z exchange diagrams. The Higgs exchange is negligible because the electron mass is very small. The analytic cross section formula in Born approximation can be found, for example, in Ref. [5]. The experimental data are compared with the SM prediction in Chap. 6 [7]. The agreement is very good. Note that the sum of all three exchange amplitudes has a better high energy behaviour. This is due to cancellations among the amplitudes implied by gauge invariance, connected to the fact that the theory is renormalizable (the crosssection can be seen as a contribution to the imaginary part of the $e^+e^- \rightarrow e^+e^-$ amplitude).

The quartic gauge coupling is proportional to $g^2 \epsilon_{ABC} W^B W^C \epsilon_{ADE} W^D W^E$. Thus in the term with $A = 3$ we have four charged W's. For $A = 1$ or two we have two charged W's and 2 W^3 's, each W_3 being a combination of γ and Z according to Eq. (3.13). With a little algebra the quartic vertex can be cast in the form:

$$V_{WWVV} = ig_{WWVV} [2g_{\mu\nu}g_{\lambda\rho} - g_{\mu\lambda}g_{\nu\rho} - g_{\mu\rho}g_{\nu\lambda}], \tag{3.37}$$

where, μ and ν refer to W^+W^+ in the $4W$ vertex and to VV in the $WWVV$ case and:

$$g_{WWWW} = g^2, \quad g_{WW\gamma\gamma} = -e^2, \quad g_{WW\gamma Z} = -eg \cos \theta_W, \quad g_{WWZZ} = -g^2 \cos^2 \theta_W. \quad (3.38)$$

In order to obtain these result for the vertex the reader must duly take into account the factor of $-1/4$ in front of $F_{\mu\nu}^2$ in the lagrangian and the statistical factors which are equal to two for each pair of identical particles (like W^+W^+ or $\gamma\gamma$, for example). The quartic coupling, being quadratic in g , hence small, could not be directly tested so far.

3.5 The Higgs Sector

We now turn to the Higgs sector of the EW lagrangian. The Higgs lagrangian is specified by the gauge principle and the requirement of renormalizability to be

$$\mathcal{L}_{\text{Higgs}} = (D_\mu \phi)^\dagger (D^\mu \phi) - V(\phi^\dagger \phi) - \bar{\psi}_L \Gamma \psi_R \phi - \bar{\psi}_R \Gamma^\dagger \psi_L \phi^\dagger, \quad (3.39)$$

where ϕ is a column vector including all Higgs fields; it transforms as a reducible representation of the gauge group. The quantities Γ (which include all coupling constants) are matrices that make the Yukawa couplings invariant under the Lorentz and gauge groups. Without loss of generality, here and in the following, we take Γ to be γ_5 -free. The potential $V(\phi^\dagger \phi)$, symmetric under $SU(2) \otimes U(1)$, contains, at most, quartic terms in ϕ so that the theory is renormalizable:

$$V(\phi^\dagger \phi) = -\mu^2 \phi^\dagger \phi + \frac{1}{2} \lambda (\phi^\dagger \phi)^2 \quad (3.40)$$

As discussed in Chap.2, spontaneous symmetry breaking is induced if the minimum of V , which is the classical analogue of the quantum mechanical vacuum state (both are the states of minimum energy), is obtained for non-vanishing ϕ values. Precisely, we denote the vacuum expectation value (VEV) of ϕ , i.e. the position of the minimum, by v (which is a doublet):

$$\langle 0 | \phi(x) | 0 \rangle = v = \begin{pmatrix} 0 \\ v \end{pmatrix} \neq 0. \quad (3.41)$$

The reader should be careful that the same symbol is used for the doublet and the only non zero component of the same doublet. The fermion mass matrix is obtained from the Yukawa couplings by replacing $\phi(x)$ by v :

$$M = \bar{\psi}_L \mathcal{M} \psi_R + \bar{\psi}_R \mathcal{M}^\dagger \psi_L, \quad (3.42)$$

with

$$\mathcal{M} = \Gamma \cdot v . \quad (3.43)$$

In the MSM, where all left fermions ψ_L are doublets and all right fermions ψ_R are singlets, only Higgs doublets can contribute to fermion masses. There are enough free couplings in Γ , so that one single complex Higgs doublet is indeed sufficient to generate the most general fermion mass matrix. It is important to observe that by a suitable change of basis we can always make the matrix \mathcal{M} Hermitian and diagonal. In fact, we can make separate unitary transformations on ψ_L and ψ_R according to

$$\psi'_L = U \psi_L, \quad \psi'_R = W \psi_R \quad (3.44)$$

and consequently

$$\mathcal{M} \rightarrow \mathcal{M}' = U^\dagger \mathcal{M} W . \quad (3.45)$$

This transformation does not alter the structure of the fermion couplings in $\mathcal{L}_{\text{symm}}$ (because both the kinetic terms and the couplings to gauge bosons do not mix L and R spinors) except that it leads to the phenomenon of mixing, as we shall see in Sect. (3.6).

If only one Higgs doublet is present, the change of basis that makes \mathcal{M} diagonal will at the same time diagonalize the fermion–Higgs Yukawa couplings. Thus, in this case, no flavour-changing neutral Higgs vertices are present. This is not true, in general, when there are several Higgs doublets. But one Higgs doublet for each electric charge sector i.e. one doublet coupled only to u -type quarks, one doublet to d -type quarks, one doublet to charged leptons (and possibly one for neutrino Dirac masses) would also be all right, because the mass matrices of fermions with different charges are diagonalized separately. For several Higgs doublets in a given charge sector it is also possible to generate CP violation by complex phases in the Higgs couplings. In the presence of six quark flavours, this CP-violation mechanism is not necessary. In fact, at the moment, the simplest model with only one Higgs doublet seems adequate for describing all observed phenomena.

We now consider the gauge-boson masses and their couplings to the Higgs. These effects are induced by the $(D_\mu \phi)^\dagger (D^\mu \phi)$ term in $\mathcal{L}_{\text{Higgs}}$ (Eq. (3.39)), where

$$D_\mu \phi = \left[\partial_\mu + ig \sum_{A=1}^3 t^A W_\mu^A + ig'(Y/2) B_\mu \right] \phi . \quad (3.46)$$

Here t^A and $Y/2$ are the $SU(2) \otimes U(1)$ generators in the reducible representation spanned by ϕ . Not only doublets but all non-singlet Higgs representations can

contribute to gauge-boson masses. The condition that the photon remains massless is equivalent to the condition that the vacuum is electrically neutral:

$$Q|v\rangle = (t^3 + \frac{1}{2}Y)|v\rangle = 0. \quad (3.47)$$

We now explicitly consider the case of a single Higgs doublet:

$$\phi = \begin{pmatrix} \phi^+ \\ \phi^0 \end{pmatrix}, \quad v = \begin{pmatrix} 0 \\ v \end{pmatrix}, \quad (3.48)$$

The charged W mass is given by the quadratic terms in the W field arising from $\mathcal{L}_{\text{Higgs}}$, when $\phi(x)$ is replaced by v in Eq. (3.41). By recalling Eq. (3.10), we obtain

$$m_W^2 W_\mu^+ W^{-\mu} = g^2 |(t^+ v/\sqrt{2})|^2 W_\mu^+ W^{-\mu}, \quad (3.49)$$

whilst for the Z mass we get [recalling Eqs. (3.12–3.14)]

$$\frac{1}{2}m_Z^2 Z_\mu Z^\mu = |[g \cos \theta_W t^3 - g' \sin \theta_W (Y/2)]v|^2 Z_\mu Z^\mu, \quad (3.50)$$

where the factor of 1/2 on the left-hand side is the correct normalization for the definition of the mass of a neutral field. By using Eq. (3.47), relating the action of t^3 and $Y/2$ on the vacuum v , and Eqs. (3.16), we obtain

$$\frac{1}{2}m_Z^2 = (g \cos \theta_W + g' \sin \theta_W)^2 |t^3 v|^2 = (g^2 / \cos^2 \theta_W) |t^3 v|^2. \quad (3.51)$$

For a Higgs doublet, as in Eq. (3.48), we have

$$|t^+ v|^2 = v^2, \quad |t^3 v|^2 = 1/4 v^2, \quad (3.52)$$

so that

$$m_W^2 = 1/2 g^2 v^2, \quad m_Z^2 = 1/2 g^2 v^2 / \cos^2 \theta_W. \quad (3.53)$$

Note that by using Eq. (3.19) we obtain

$$v = 2^{-3/4} G_F^{-1/2} = 174.1 \text{ GeV}. \quad (3.54)$$

It is also evident that for Higgs doublets

$$\rho_0 = \frac{m_W^2}{m_Z^2 \cos^2 \theta_W} = 1. \quad (3.55)$$

This relation is typical of one or more Higgs doublets and would be spoiled by the existence of Higgs triplets etc. In general,

$$\rho_0 = \frac{\sum_i ((t_i)^2 - (t_i^3)^2 + t_i) v_i^2}{\sum_i 2(t_i^3)^2 v_i^2} \quad (3.56)$$

for several Higgs bosons with VEVs v_i , weak isospin t_i , and z -component t_i^3 . These results are valid at the tree level and are modified by calculable EW radiative corrections, as discussed in Sect. (3.7).

The measured values of the W and Z masses are [5, 8] (see Chap. 6):

$$m_W = 80.398 \pm 0.025 \text{ GeV}, \quad m_Z = 91.1875 \pm 0.0021 \text{ GeV}. \quad (3.57)$$

In the minimal version of the SM only one Higgs doublet is present. Then the fermion–Higgs couplings are in proportion to the fermion masses. In fact, from the Yukawa couplings $g_{\phi \bar{f} f} (\bar{f}_L \phi f_R + h.c.)$, the mass m_f is obtained by replacing ϕ by v , so that $m_f = g_{\phi \bar{f} f} v$. In the minimal SM three out of the four Hermitian fields are removed from the physical spectrum by the Higgs mechanism and become the longitudinal modes of W^+ , W^- , and Z . The fourth neutral Higgs is physical and should be found. If more doublets are present, two more charged and two more neutral Higgs scalars should be around for each additional doublet.

The couplings of the physical Higgs H can be simply obtained from $\mathcal{L}_{\text{Higgs}}$, by the replacement (the remaining three hermitian fields correspond to the would be Goldstone bosons that become the longitudinal modes of W^\pm and Z):

$$\phi(x) = \begin{pmatrix} \phi^+(x) \\ \phi^0(x) \end{pmatrix} \rightarrow \begin{pmatrix} 0 \\ v + (H/\sqrt{2}) \end{pmatrix}, \quad (3.58)$$

[so that $(D_\mu \phi)^\dagger (D^\mu \phi) = 1/2(\partial_\mu H)^2 + \dots$], with the results

$$\begin{aligned} \mathcal{L}[H, W, Z] = & g^2 \frac{v}{\sqrt{2}} W_\mu^+ W^{-\mu} H + \frac{g^2}{4} W_\mu^+ W^{-\mu} H^2 + \\ & + g^2 \frac{v}{2\sqrt{2} \cos^2 \theta_W} Z_\mu Z^\mu H + \frac{g^2}{8 \cos^2 \theta_W} Z_\mu Z^\mu H^2. \end{aligned} \quad (3.59)$$

Note that the trilinear couplings are nominally of order g^2 , but the adimensional coupling constant is actually of order g if we express the couplings in terms of the

masses according to Eqs. (3.53):

$$\begin{aligned} \mathcal{L}[H, W, Z] = & gm_W W_\mu^+ W^{-\mu} H + \frac{g^2}{4} W_\mu^+ W^{-\mu} H^2 + \\ & + \frac{gm_Z}{2 \cos^2 \theta_W} Z_\mu Z^\mu H + \frac{g^2}{8 \cos^2 \theta_W} Z_\mu Z^\mu H^2 . \end{aligned} \quad (3.60)$$

Thus the trilinear couplings of the Higgs to the gauge bosons are also proportional to the masses. The quadrilinear couplings are genuinely of order g^2 . Recall that to go from the lagrangian to the Feynman rules for the vertices the statistical factors must be taken into account: for example, the Feynman rule for the $ZZHH$ vertex is $ig_{\mu\nu}g^2/2 \cos^2 \theta_W$.

The generic coupling of H to a fermion of type f is given by (after diagonalization):

$$\mathcal{L}[H, \bar{\psi}, \psi] = \frac{gf}{\sqrt{2}} \bar{\psi} \psi H, \quad (3.61)$$

with

$$\frac{gf}{\sqrt{2}} = \frac{m_f}{\sqrt{2}v} = 2^{1/4} G_F^{1/2} m_f . \quad (3.62)$$

The Higgs self couplings are obtained from the potential in Eq. (3.40) by the replacement in Eq. (3.58). Given that, from the minimum condition:

$$v = \sqrt{\frac{\mu^2}{\lambda}} \quad (3.63)$$

one obtains:

$$V = -\mu^2 \left(v + \frac{H}{\sqrt{2}}\right)^2 + \frac{\mu^2}{2v^2} \left(v + \frac{H}{\sqrt{2}}\right)^4 = -\frac{\mu^2 v^2}{2} + \mu^2 H^2 + \frac{\mu^2}{\sqrt{2}v} H^3 + \frac{\mu^2}{8v^2} H^4 \quad (3.64)$$

The constant term can be omitted in our context. We see that the Higgs mass is positive (compare with Eq. (3.40)) and is given by:

$$m_H^2 = 2\mu^2 = 2\lambda v^2 \quad (3.65)$$

We see that for $\sqrt{\lambda} \sim o(1)$ the Higgs mass should be of the order of the weak scale.

The difficulty of the Higgs search is due to the fact that it is heavy and coupled in proportion to mass: it is a heavy particle that must be radiated by another heavy particle. So a lot of phase space and luminosity is needed. At LEP2 the main process for Higgs production was the Higgs-strahlung process $e^+e^- \rightarrow ZH$ shown in

Fig. 3.5 Higgs production diagrams in Born approximation: **(a)** The Higgs-strahlung process $e^+e^- \rightarrow ZH$, **(b)** the WW fusion process $e^+e^- \rightarrow H\nu\bar{\nu}$

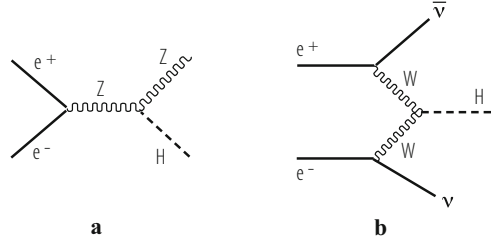


Fig. 3.5 [9]. The alternative process $e^+e^- \rightarrow H\nu\bar{\nu}$, via WW fusion, also shown in Fig. 3.5 [10], has a smaller crosssection at LEP2 energies but would become important, even dominant at higher energy e^+e^- colliders, like the ILC or CLIC (the corresponding ZZ fusion process has a much smaller crosssection). The analytic formulae for the crosssections of both processes can be found, for example, in [11]. The direct experimental limit on m_H from LEP2 is $m_H \gtrsim 114$ GeV at 95% c.l. (see Chap. 6).

3.6 The CKM Matrix

Weak charged currents are the only tree level interactions in the SM that change flavour: for example, by emission of a W an up-type quark is turned into a down-type quark, or a ν_l neutrino is turned into a l^- charged lepton (all fermions are left-handed). If we start from an up quark that is a mass eigenstate, emission of a W turns it into a down-type quark state d' (the weak isospin partner of u) that in general is not a mass eigenstate. The mass eigenstates and the weak eigenstates do not coincide and a unitary transformation connects the two sets:

$$D' = \begin{pmatrix} d' \\ s' \\ b' \end{pmatrix} = V \begin{pmatrix} d \\ s \\ b \end{pmatrix} = VD \quad (3.66)$$

V is the Cabibbo-Kobayashi-Maskawa (CKM) matrix [12] (and similarly we can denote by U the column vector of the three up quark mass eigenstates). Thus in terms of mass eigenstates the charged weak current of quarks is of the form:

$$J_\mu^+ \propto \bar{U} \gamma_\mu (1 - \gamma_5) t^+ V D \quad (3.67)$$

where

$$V = U_u^\dagger U_d \quad (3.68)$$

Here U_u and U_d are the unitary matrices that operate on left-handed doublets in the diagonalization of the u and d quarks, respectively (see Eq.(3.44)). Since V is unitary (i.e. $VV^\dagger = V^\dagger V = 1$) and commutes with T^2 , T_3 and Q (because all d-type quarks have the same isospin and charge), the neutral current couplings are diagonal both in the primed and unprimed basis (if the down-type quark terms in the Z current are written in terms of weak isospin eigenvectors as $\bar{D}'\Gamma D'$, then by changing basis we get $\bar{D}V^\dagger\Gamma VD$ and V and Γ commute because, as seen from Eq.(3.23), Γ is made of Dirac matrices and of T_3 and Q generator matrices). It follows that $\bar{D}'\Gamma D' = \bar{D}\Gamma D$. This is the GIM mechanism [13] that ensures natural flavour conservation of the neutral current couplings at the tree level.

For N generations of quarks, V is a $N \times N$ unitary matrix that depends on N^2 real numbers (N^2 complex entries with N^2 unitarity constraints). However, the $2N$ phases of up- and down-type quarks are not observable. Note that an overall phase drops away from the expression of the current in Eq.(3.67), so that only $2N - 1$ phases can affect V . In total, V depends on $N^2 - 2N + 1 = (N - 1)^2$ real physical parameters. A similar counting gives $N(N - 1)/2$ as the number of independent parameters in an orthogonal $N \times N$ matrix. This implies that in V we have $N(N - 1)/2$ mixing angles and $(N - 1)^2 - N(N - 1)/2 = (N - 1)(N - 2)/2$ phases: for $N = 2$ one mixing angle (the Cabibbo angle θ_C) and no phases, for $N = 3$ three angles (θ_{12} , θ_{13} and θ_{23}) and one phase φ etc.

Given the experimental near diagonal structure of V a convenient parametrisation is the one proposed by Maiani [14]. It can be cast in the form of a product of three independent 2×2 block matrices (s_{ij} and c_{ij} are shorthands for $\sin\theta_{ij}$ and $\cos\theta_{ij}$):

$$V = \begin{pmatrix} 1 & 0 & 0 \\ 0 & c_{23} & s_{23} \\ 0 & -s_{23} & c_{23} \end{pmatrix} \begin{pmatrix} c_{13} & 0 & s_{13}e^{i\varphi} \\ 0 & 1 & 0 \\ -s_{13}e^{-i\varphi} & 0 & c_{13} \end{pmatrix} \begin{pmatrix} c_{12} & s_{12} & 0 \\ -s_{12} & c_{12} & 0 \\ 0 & 0 & 1 \end{pmatrix}. \quad (3.69)$$

The advantage of this parametrization is that the three mixing angles are of different orders of magnitude. In fact, from experiment we know that $s_{12} \equiv \lambda$, $s_{23} \sim o(\lambda^2)$ and $s_{13} \sim o(\lambda^3)$, where $\lambda = \sin\theta_C$ is the sine of the Cabibbo angle, and, as order of magnitude, s_{ij} can be expressed in terms of small powers of λ . More precisely, following Wolfenstein [15] one can set:

$$s_{12} \equiv \lambda, \quad s_{23} = A\lambda^2, \quad s_{13}e^{-i\phi} = A\lambda^3(\rho - i\eta) \quad (3.70)$$

As a result, by neglecting terms of higher order in λ one can write down:

$$V = \begin{bmatrix} V_{ud} & V_{us} & V_{ub} \\ V_{cd} & V_{cs} & V_{cb} \\ V_{td} & V_{ts} & V_{tb} \end{bmatrix} \sim \begin{bmatrix} 1 - \frac{\lambda^2}{2} & \lambda & A\lambda^3(\rho - i\eta) \\ -\lambda & 1 - \frac{\lambda^2}{2} & A\lambda^2 \\ A\lambda^3(1 - \rho - i\eta) & -A\lambda^2 & 1 \end{bmatrix} + o(\lambda^4). \quad (3.71)$$

It has become customary to make the replacement $\rho, \eta \rightarrow \bar{\rho}, \bar{\eta}$ with:

$$\rho - i\eta = \frac{\bar{\rho} - i\bar{\eta}}{\sqrt{1 - \lambda^2}} \sim (\bar{\rho} - i\bar{\eta})(1 + \lambda^2/2 + \dots). \quad (3.72)$$

Present values of the CKM parameters as obtained from experiment are [16] [17] (a survey of the current status of the CKM parameters can also be found in Ref. [5]):

$$\begin{aligned} \lambda &= 0.2258 \pm 0.0014 \\ A &= 0.818 \pm 0.016 \\ \bar{\rho} &= 0.164 \pm 0.029; \quad \bar{\eta} = 0.340 \pm 0.017 \end{aligned} \quad (3.73)$$

A more detailed discussion of the experimental data is given in Chap. 10.

In the SM the non vanishing of the η parameter (related to the phase φ in Eqs. 3.69 and 3.70) is the only source of CP violation. Unitarity of the CKM matrix V implies relations of the form $\sum_a V_{ba} V_{ca}^* = \delta_{bc}$. In most cases these relations do not imply particularly instructive constraints on the Wolfenstein parameters. But when the three terms in the sum are of comparable magnitude we get interesting information. The three numbers which must add to zero form a closed triangle in the complex plane, with sides of comparable length. This is the case for the t-u triangle (unitarity triangle) shown in Fig. 3.6 (or, what is equivalent in first approximation, for the d-b triangle):

$$V_{td} V_{ud}^* + V_{ts} V_{us}^* + V_{tb} V_{ub}^* = 0 \quad (3.74)$$

All terms are of order λ^3 . For $\eta = 0$ the triangle would flatten down to vanishing area. In fact the area of the triangle, J of order $J \sim \eta A^2 \lambda^6$, is the Jarlskog invariant [18] (its value is independent of the parametrization). In the SM all CP violating observables must be proportional to J , hence to the area of the triangle or to η . A direct and by now very solid evidence for J non vanishing is obtained from the measurements of ϵ and ϵ' in K decay. Additional direct evidence is being obtained from the experiments on B decays at beauty factories and at the TeVatron where the angles β (the most precisely measured), α and γ have been determined. Together with the available information on the magnitude of the sides all the measurements

Fig. 3.6 The unitarity triangle corresponding to Eq. (3.74)

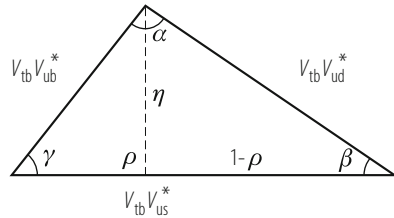
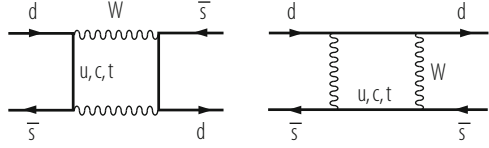


Fig. 3.7 Box diagrams describing $K^0 - \bar{K}^0$ mixing at the quark level at 1-loop



are in good agreement with the predictions from the SM unitary triangle [16, 17] (see Chap. 10).

As we have discussed, due to the GIM mechanism, there are no flavour changing neutral current (FCNC) transitions at tree level in the SM. Transitions with $|\Delta F| = 1, 2$ are induced at one loop level. In particular, meson mixing, i.e. $M \rightarrow \bar{M}$ off diagonal $|\Delta F| = 2$ mass matrix elements (with $M = K, D$ or B neutral mesons), are obtained from box diagrams. For example, in the case of $K^0 - \bar{K}^0$ mixing the relevant transition is $\bar{s}d \rightarrow s\bar{d}$ (see Fig. 3.7). In the internal quark lines all up-type quarks are exchanged. In the amplitude, two vertices and the connecting propagator (with virtual four momentum p_μ) at one side contribute a factor ($u_i = u, c, t$):

$$F_{GIM} = \sum_i V_{uis}^* \frac{1}{\not{p} - m_{ui}} V_{uid}, \quad (3.75)$$

which, in the limit of equal m_{ui} , is clearly vanishing due to the unitarity of the CKM matrix V . Thus the result is proportional to mass differences. For $K^0 - \bar{K}^0$ mixing the contribution of virtual u quarks is negligible due to the small value of m_u and the contribution of the t quark is also small due to the mixing factors $V_{ts}^* V_{td} \sim o(A^2 \lambda^5)$. The dominant c quark contribution to the real part of the box diagram quark-level amplitude is approximately of the form (see, for example, [19]):

$$Re H_{box} = \frac{G_F^2}{16\pi^2} m_c^2 Re(V_{cs}^* V_{cd})^2 \eta_1 O^{\Delta s=2}, \quad (3.76)$$

where $\eta_1 \sim 0.85$ is a QCD correction factor and $O^{\Delta s=2} = \bar{d}_L \gamma_\mu s_L \bar{s}_L \gamma_\mu d_L$ is the 4-quark dimension six relevant operator. To obtain the $K^0 - \bar{K}^0$ mixing its matrix element between meson states must be taken which is parametrized in terms of a “ B_K parameter” which is defined in such a way that $B_K = 1$ for vacuum state insertion between the two currents:

$$\langle K^0 | O^{\Delta s=2} | \bar{K}^0 \rangle = \frac{16}{3} f_K m_K^2 B_K, \quad (3.77)$$

where $f_K \sim 113 MeV$ is the kaon pseudoscalar constant. Clearly to the charm contribution in Eq. (3.76) non perturbative additional contributions must be added, some of them of $o(m_K^2/m_c^2)$, because the smallness of m_c makes a completely partonic dominance inadequate. In particular, B_K is best evaluated by QCD lattice simulations. In Eq. (3.76) the factor $o(m_c^2/m_W^2)$ is the “GIM suppression” factor

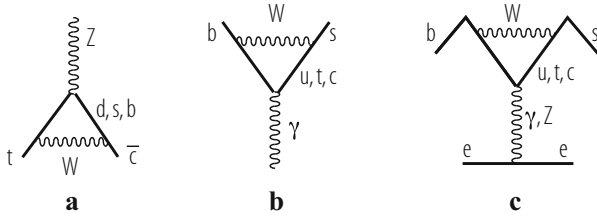


Fig. 3.8 Examples of $|\Delta F| = 1$ transitions at the quark level at 1-loop: (a) Diagram for a $Z \rightarrow t \bar{c}$ vertex, (b) $b \rightarrow s \gamma$, (c) a “penguin” diagram for $b \rightarrow s e^+ e^-$

($1/m_W^2$ is hidden in G_F according to Eq.(3.19)). For B mixing the dominant contribution is from the t quark. In this case, the partonic dominance is more realistic and the GIM factor $o(m_t^2/m_W^2)$ is actually larger than one.

All sorts of transitions with $|\Delta F| = 1$ are also induced at loop level. For example, an effective vertex $Z \rightarrow t \bar{c}$, which does not exist at tree level, is generated at 1-loop (see Fig. 3.8). Similarly, transitions involving photons or gluons are also possible, like $t \rightarrow c g$ or $b \rightarrow s \gamma$ (Fig. 3.8) or $b \rightarrow s g$. For light fermion exchange in the loop the GIM suppression is also effective in $|\Delta F| = 1$ amplitudes. For example, analogous leptonic transitions like $\mu \rightarrow e \gamma$ or $\tau \rightarrow \mu \gamma$ also exist but are extremely small in the SM because the tiny neutrino masses enter in the GIM suppression factor. But new physics effects could well make these rare processes accessible to experiments in the near future. The external Z, photon or gluon can be attached to a pair of light fermions, giving rise to an effective four fermion operator, as in “penguin diagrams” like the one shown in Fig. 3.8 for $b \rightarrow s l^+ l^-$. The inclusive rate $B \rightarrow X_s \gamma$ with X_s a hadronic state containing a unit of strangeness corresponding to an s-quark, has been precisely measured. The world average result for the branching ratio with $E_\gamma > 1.6$ GeV is [5]:

$$B(B \rightarrow X_s \gamma)_{exp} = (3.55 \pm 0.26) \cdot 10^{-4}. \quad (3.78)$$

The theoretical prediction for this inclusive process is to a large extent free of uncertainties from hadronisation effects and is accessible to perturbation theory as the b-quark is heavy enough. The most complete result at order α_s^2 is at present [20] (and refs. therein):

$$B(B \rightarrow X_s \gamma)_{th} = (2.98 \pm 0.26) \cdot 10^{-4}. \quad (3.79)$$

Note that the theoretical value has recently become smaller than the experimental value. The fair agreement between theory and experiment imposes stringent constraints on possible new physics effects.

3.7 Neutrino Masses

In the minimal version of the SM the right handed neutrinos ν_{iR} , which have no gauge interactions, are not present at all. With no ν_R no Dirac mass is possible for neutrinos. If lepton number conservation is also imposed, then no Majorana mass is allowed either and, as a consequence, all neutrinos are massless. But, at present, from neutrino oscillation experiments (see Chapter 11 of the present work), we know that at least 2 out of the 3 known neutrinos have non vanishing masses: the two mass squared differences measured from solar (Δm_{12}^2) and atmospheric oscillations (Δm_{23}^2) are given by $\Delta m_{12}^2 \sim 8 \cdot 10^{-5} eV^2$ and $\Delta m_{23}^2 \sim 2.5 \cdot 10^{-3}$ [21]. The absolute values of the masses are very small, with an upper limit of a fraction of eV , obtained from laboratory experiments (tritium β decay near the end point: $m_\nu \lesssim 2 eV$ [5], absence of visible neutrinoless double β decay: $|m_{ee}| \lesssim 0.3 - 0.7 eV$ (m_{ee} is a combination of neutrino masses; for a review, see, for example [22]) and from cosmological observations: $m_\nu \lesssim 0.1 - 0.7 eV$ (depending on the cosmological model assumptions) [23]. If ν_{iR} are added to the minimal model and lepton number is imposed by hand, then neutrino masses would in general appear as Dirac masses, generated by the Higgs mechanism, like for any other fermion. But, for Dirac neutrinos, to explain the extreme smallness of neutrino masses, one should allow for very small Yukawa couplings. However, we stress that, in the SM, baryon B and lepton L number conservation, which are not guaranteed by gauge symmetries (as is the case for the electric charge Q), are understood as “accidental” symmetries, due to the fact that, out of the SM fields, it is not possible to construct gauge invariant operators which are renormalizable (i.e. of operator dimension $d \leq 4$) and violate B and/or L . In fact the SM lagrangian should contain all terms allowed by gauge symmetry and renormalizability. The most general renormalizable lagrangian, built from the SM fields, compatible with the SM gauge symmetry, in absence of ν_{iR} , is automatically B and L conserving. But in presence of ν_{iR} , this is no more true and the right handed Majorana mass term is allowed:

$$M_{RR} = \bar{\nu}_{iR}^c M_{ij} \nu_{jR} = \nu_{iR}^T C M_{ij} \nu_{jR} , \quad (3.80)$$

where $\nu_{iR}^c = C \bar{\nu}_{iR}^T$ is the charge conjugated neutrino field and C is the charge conjugation matrix in Dirac spinor space. The Majorana mass term is an operator of dimension $d = 3$ with $\Delta L = 2$. Since the ν_{iR} are gauge singlets the Majorana mass M_{RR} is fully allowed by the gauge symmetry and a coupling with the Higgs is not needed to generate this type of mass. As a consequence, the entries of the mass matrix M_{ij} do not need to be of the order of the EW symmetry breaking scale v and could be much larger. If one starts from the Dirac and RR Majorana mass terms for neutrinos, the resulting mass matrix, in the L, R space, has the form:

$$m_\nu = \begin{bmatrix} 0 & m_D \\ m_D & M \end{bmatrix} \quad (3.81)$$

where m_D and M are the Dirac and Majorana mass matrices (M is the matrix M_{ij} in Eq. (3.80)). The corresponding eigenvalues are three very heavy neutrinos with masses of order M and three light neutrinos with masses

$$m_\nu = -m_D^T M^{-1} m_D, \quad (3.82)$$

which are possibly very small if M is large enough. This is the see-saw mechanism for neutrino masses [24]. Note that if no ν_{iR} exist a Majorana mass term could still be built out of ν_{jL} . But ν_{jL} have weak isospin 1/2, being part of the left handed lepton doublet l . Thus, the left handed Majorana mass term has total weak isospin equal to one and needs two Higgs fields to make a gauge invariant term. The resulting mass term:

$$O_5 = \lambda l_i^T \lambda_{ij} l_j H H / M, \quad (3.83)$$

with M a large scale (a priori comparable to the scale of M_{RR}) and λ a dimensionless coupling generically of $o(1)$, is a non renormalizable operator of dimension 5. The corresponding mass terms are of the order $m_\nu \sim \lambda v^2 / M$, hence of the same generic order of the light neutrino masses from Eq. (3.82).

In conclusion, neutrino masses are believed to be small because neutrinos are Majorana particles with masses inversely proportional to the large scale M of energy where L non conservation is induced. It is interesting that the observed magnitudes of the mass squared splittings of neutrinos are well compatible with a scale M remarkably close to the Grand Unification scale, where in fact L non conservation is naturally expected.

In the previous Section we have discussed flavour mixing for quarks. But, clearly, given that non vanishing neutrino masses have been established, a similar mixing matrix is also introduced in the leptonic sector, but will not be discussed here (see Chapter 11).

3.8 Renormalization of the Electroweak Theory

The Higgs mechanism gives masses to the Z, the W^\pm and to fermions while the lagrangian density is still symmetric. In particular the gauge Ward identities and the symmetric form of the gauge currents are preserved. The validity of these relations is an essential ingredient for renormalizability. In the previous Sections we have specified the Feynman vertices in the “unitary” gauge where only physical particles appear. However, as discussed in Chap. 2, in this gauge the massive gauge boson propagator would have a bad ultraviolet behaviour:

$$W_{\mu\nu} = \frac{-g_{\mu\nu} + \frac{q_\mu q_\nu}{m_W^2}}{q^2 - m_W^2}. \quad (3.84)$$

A formulation of the standard EW theory with good apparent ultraviolet behaviour can be obtained by introducing the renormalizable or R_ξ gauges, in analogy with the abelian case discussed in detail in Chap. 2. One parametrizes the Higgs doublet as:

$$\phi = \begin{pmatrix} \phi^+ \\ \phi^0 \end{pmatrix} = \begin{pmatrix} \phi_1 + i\phi_2 \\ \phi_3 + i\phi_4 \end{pmatrix} = \begin{pmatrix} -iw^+ \\ v + \frac{H+iz}{\sqrt{2}} \end{pmatrix}, \quad (3.85)$$

and similarly for ϕ^\dagger , where w^- appears. The scalar fields w^\pm and z are the pseudo Goldstone bosons associated with the longitudinal modes of the physical vector bosons W^\pm and Z . The R_ξ gauge fixing lagrangian has the form:

$$\Delta\mathcal{L}_{GF} = -\frac{1}{\xi}|\partial^\mu W_\mu - \xi m_W w|^2 - \frac{1}{2\eta}(\partial^\mu Z_\mu - \eta m_Z z)^2 - \frac{1}{2\alpha}(\partial^\mu A_\mu)^2. \quad (3.86)$$

The W^\pm and Z propagators, as well as those of the scalars w^\pm and z , have exactly the same general forms as for the abelian case in Eqs. (67)–(69) of Chap. 2, with parameters ξ and η , respectively (and the pseudo Goldstone bosons w^\pm and z have masses ξm_W and ηm_Z). In general, a set of associated ghost fields must be added, again in direct analogy with the treatment of R_ξ gauges in the abelian case of Chap. 2. The complete Feynman rules for the standard EW theory can be found in a number of textbooks (see, for example, [25]).

The pseudo Goldstone bosons w^\pm and z are directly related to the longitudinal helicity states of the corresponding massive vector bosons W^\pm and Z . This correspondence materializes in a very interesting “equivalence theorem”: at high energies of order E the amplitude for the emission of one or more longitudinal gauge bosons V_L (with $V = W, Z$) becomes equal (apart from terms down by powers of m_V/E) to the amplitude where each longitudinal gauge boson is replaced by the corresponding Goldstone field w^\pm or z [26]. For example, consider top decay with a longitudinal W in the final state: $t \rightarrow bW_L^+$. The equivalence theorem asserts that we can compute the dominant contribution to this rate from the simpler $t \rightarrow bw^+$ matrix element:

$$\Gamma(t \rightarrow bW_L^+) = \Gamma(t \rightarrow bw^+)[1 + o(m_W^2/m_t^2)]. \quad (3.87)$$

In fact one finds:

$$\Gamma(t \rightarrow bw^+) = \frac{h_t^2}{32\pi} m_t = \frac{G_F m_t^3}{8\pi\sqrt{2}}, \quad (3.88)$$

where $h_t = m_t/v$ is the Yukawa coupling of the top quark (numerically very close to 1), and we used $1/v^2 = 2\sqrt{2}G_F$ (see Eq. (3.54)). If we compare with Eq. (3.34), we see that this expression coincides with the total top width (i.e. including all polarizations for the W in the final state), computed at tree level, apart from terms

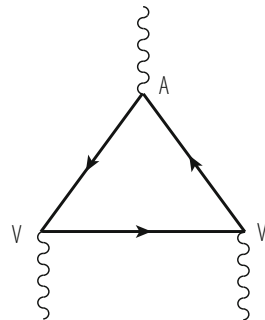
down by powers of $o(m_W^2/m_t^2)$. In fact, the longitudinal W is dominant in the final state because $h_t \gg g^2$. Similarly the equivalence theorem can be applied to find the dominant terms at large \sqrt{s} for the crosssection $e^+e^- \rightarrow W_L^+W_L^-$, or the leading contribution in the limit $m_H \gg m_V$ to the width for the decay $\Gamma(H \rightarrow VV)$.

The formalism of the R_ξ gauges is also very useful in proving that spontaneously broken gauge theories are renormalizable. In fact, the non singular behaviour of propagators at large momenta is very suggestive of the result. Nevertheless to prove it is by far not a simple matter. The fundamental theorem that in general a gauge theory with spontaneous symmetry breaking and the Higgs mechanism is renormalizable was proven by 't Hooft and Veltman [27, 28].

For a chiral theory like the SM an additional complication arises from the existence of chiral anomalies. But this problem is avoided in the SM because the quantum numbers of the quarks and leptons in each generation imply a remarkable (and, from the point of view of the SM, mysterious) cancellation of the anomaly, as originally observed in Ref. [29]. In quantum field theory one encounters an anomaly when a symmetry of the classical lagrangian is broken by the process of quantization, regularization and renormalization of the theory. Of direct relevance for the EW theory is the Adler-Bell-Jackiw (ABJ) chiral anomaly [30]. The classical lagrangian of a theory with massless fermions is invariant under a U(1) chiral transformations $\psi' = e^{i\gamma_5\theta}\psi$. The associated axial Noether current is conserved at the classical level. But, at the quantum level, chiral symmetry is broken due to the ABJ anomaly and the current is not conserved. The chiral breaking is produced by a clash between chiral symmetry, gauge invariance and the regularization procedure.

The anomaly is generated by triangular fermion loops with one axial and two vector vertices (Fig. 3.9). For example, for the Z the axial coupling is proportional to the third component of weak isospin t_3 , while the vector coupling is proportional to a linear combination of t_3 and the electric charge Q . Thus in order for the chiral anomaly to vanish all traces of the form $tr\{t_3QQ\}$, $tr\{t_3t_3Q\}$, $tr\{t_3t_3t_3\}$ (and also $tr\{t_+t_-t_3\}$ when charged currents are also included) must vanish, where the trace is extended over all fermions in the theory that can circulate in the loop. Now all these traces happen to vanish for each fermion family separately. For example take $tr\{t_3QQ\}$. In one family there are, with $t_3 = +1/2$, three colours of up quarks with

Fig. 3.9 Triangle diagram that generates the ABJ anomaly



charge $Q = +2/3$ and one neutrino with $Q = 0$ and, with $t_3 = -1/2$, three colours of down quarks with charge $Q = -1/3$ and one l^- with $Q = -1$. Thus we obtain $tr\{t_3 Q Q\} = 1/2 \cdot 3 \cdot 4/9 - 1/2 \cdot 3 \cdot 1/9 - 1/2 \cdot 1 = 0$. This impressive cancellation suggests an interplay among weak isospin, charge and colour quantum numbers which appears as a miracle from the point of view of the low energy theory but is in fact understandable from the point of view of the high energy theory. For example, in Grand Unified Theories (GUTs) (for reviews, see, for example, [31]) there are similar relations where charge quantization and colour are related: in the five of SU(5) we have the content $(d, d, d, e^+, \bar{\nu})$ and the charge generator has a vanishing trace in each SU(5) representation (the condition of unit determinant, represented by the letter S in the SU(5) group name, translates into zero trace for the generators). Thus the charge of d quarks is $-1/3$ of the positron charge because there are three colours. A whole family fits perfectly in one 16 of SO(10) which is anomaly free. So GUTs can naturally explain the cancellation of the chiral anomaly.

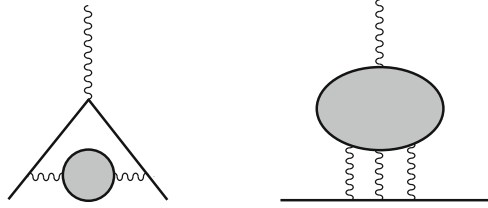
An important implication of chiral anomalies together with the topological properties of the vacuum in non abelian gauge theories is that the conservation of the charges associated to baryon (B) and lepton (L) numbers is broken by the anomaly [32], so that B and L conservation is actually violated in the standard electroweak theory (but B-L remains conserved). B and L are conserved to all orders in the perturbative expansion but the violation occurs via non perturbative instanton effects [33] (the amplitude is proportional to the typical non perturbative factor $\exp -c/g^2$, with c a constant and g the SU(2) gauge coupling). The corresponding effect is totally negligible at zero temperature T , but becomes relevant at temperatures close to the electroweak symmetry breaking scale, precisely at $T \sim o(TeV)$. The non conservation of B+L and the conservation of B-L near the weak scale plays a role in the theory of baryogenesis that quantitatively aims at explaining the observed matter antimatter asymmetry in the Universe (for a recent review, see, for example, [34]; see also Chap. 9).

3.9 QED Tests: Lepton Anomalous Magnetic Moments

The most precise tests of the electroweak theory apply to the QED sector. Here we discuss some recent developments. The anomalous magnetic moments of the electron and of the muon are among the most precise measurements in the whole of physics. The magnetic moment $\vec{\mu}$ and the spin \vec{S} are related by $\vec{\mu} = -g e \vec{S} / 2m$, where g is the gyromagnetic ratio ($g = 2$ for a pointlike Dirac particle). The quantity $a = (g - 2)/2$ measures the anomalous magnetic moment of the particle. Recently there have been new precise measurements of a_e and a_μ for the electron [35] and the muon [36]:

$$a_e^{exp} = 11596521808.5(7.6) \cdot 10^{-13}, \quad a_\mu^{exp} = 11659208.0(6.3) \cdot 10^{-10}. \quad (3.89)$$

Fig. 3.10 The hadronic contributions to the anomalous magnetic moment: vacuum polarization (left) and light by light scattering (right)



The theoretical calculations in general contain a pure QED part plus the sum of hadronic and weak contribution terms:

$$a = a^{QED} + a^{hadronic} + a^{weak} = \sum_i C_i \left(\frac{\alpha}{\pi}\right)^i + a^{hadronic} + a^{weak}. \quad (3.90)$$

The QED part has been computed analytically for $i = 1, 2, 3$, while for $i = 4$ there is a numerical calculation with an error (see, for example, [38] and refs therein). Some terms for $i = 5$ have also been estimated for the muon case. The hadronic contribution is from vacuum polarization insertions and from light by light scattering diagrams (see Fig. 3.10). The weak contribution is from W or Z exchange.

For the electron case the weak contribution is essentially negligible and the hadronic term ($a_e^{hadronic} \sim (16.71 \pm 0.19) \cdot 10^{-13}$) does not introduce an important uncertainty. As a result this measurement can be used to obtain the most precise determination of the fine structure constant [37]:

$$\alpha^{-1} \sim 137.035999710(96), \quad (3.91)$$

with an uncertainty about 10 times smaller than the previous determination. However, very recently a theoretical error in the α^4 terms was corrected [39]. As a result the value of α^{-1} in Eq. (3.91) is shifted by $-6.41180(73) \cdot 10^{-7}$ (about 7σ 's). This change has a minor impact in the following discussion of the muon ($g - 2$).

In the muon case the experimental precision is less by about three orders of magnitude, but the sensitivity to new physics effects is typically increased by a factor $(m_\mu/m_e)^2 \sim 4 \cdot 10^4$ (one mass factor arises because the effective operator needs a chirality flip and the second one is because, by definition, one must factor out the Bohr magneton $e/2m$). From the theory side, the QED term (using the value of α from a_e in Eq. (3.91)), and the weak contribution are affected by small errors and are given by (all theory number are taken here from the review [40])

$$a_\mu^{QED} = (116584718.09 \pm 1.6) \cdot 10^{-11}, \quad a_\mu^{weak} = (154 \pm 2.2) \cdot 10^{-11} \quad (3.92)$$

The dominant ambiguities arise from the hadronic term. The lowest order (LO) vacuum polarization contribution can be evaluated from the measured cross sections in $e^+e^- \rightarrow \text{hadrons}$ at low energy via dispersion relations (the largest contribution is from the $\pi\pi$ final state), with the result $a_\mu^{LO} \cdot 10^{-11} = 6909 \pm 44$. The higher

order (HO) vacuum polarization contribution (from 2-loop diagrams containing an hadronic insertion) is given by: $a_\mu^{HO} \cdot 10^{-11} = -98 \pm 1$. The contribution of the light by light (LbL) scattering diagrams is estimated to be: $a_\mu^{LbL} \cdot 10^{-11} = 120 \pm 35$. Adding the above contributions up the total hadronic result is reported as:

$$a_\mu^{hadronic} = (6931 \pm 56) \cdot 10^{-11}. \quad (3.93)$$

At face value this would lead to a 3.3σ deviation from the experimental value a_μ^{exp} in Eq. (3.89):

$$a_\mu^{exp} - a_\mu^{th(e^+e^-)} = (275 \pm 84) \cdot 10^{-11}. \quad (3.94)$$

However, the error estimate on the LbL term, mainly a theoretical uncertainty, is not compelling, and it could well be somewhat larger (although probably not by as much as to make the discrepancy to completely disappear). Another puzzle is the fact that, using the conservation of the vector current (CVC) and isospin invariance, which are well established tools at low energy, a_μ^{LO} can also be evaluated from τ decays. But the results on the hadronic contribution from e^+e^- and from τ decay, nominally of comparable accuracy, do not match well, and the discrepancy would be much attenuated if one takes the τ result [41]. Since it is difficult to find a theoretical reason for the e^+e^- vs τ difference, one must conclude that there is something which is not understood either in the data or in the assessment of theoretical errors. The prevailing view is to take the e^+e^- determination as the most directly reliable, which leads to Eq. (3.94), but doubts certainly remain. Finally, we note that, given the great accuracy of the a_μ measurement and the relative importance of the non QED contributions, it is not unreasonable that a first signal of new physics can appear in this quantity.

3.10 Large Radiative Corrections to Electroweak Processes

Since the SM theory is renormalizable higher order perturbative corrections can be reliably computed. Radiative corrections are very important for precision EW tests. The SM inherits all successes of the old V-A theory of charged currents and of QED. Modern tests have focussed on neutral current processes, the W mass and the measurement of triple gauge vertices. For Z physics and the W mass the state of the art computation of radiative corrections include the complete one loop diagrams and selected dominant two loop corrections. In addition some resummation techniques are also implemented, like Dyson resummation of vacuum polarization functions and important renormalization group improvements for large QED and QCD logarithms. We now discuss in more detail sets of large radiative corrections which are particularly significant (for reviews of radiative corrections for LEP1 physics, see, for example: [42]).

Even leaving aside QCD corrections, a set of important quantitative contributions to the radiative corrections arise from large logarithms [e.g. terms of the form $(\alpha/\pi \ln(m_Z/m_{f_l}))^n$ where f_l is a light fermion]. The sequences of leading and close-to-leading logarithms are fixed by well-known and consolidated techniques (β functions, anomalous dimensions, penguin-like diagrams, etc.). For example, large logarithms from pure QED effects dominate the running of α from m_e , the electron mass, up to m_Z . Similarly large logarithms of the form $[\alpha/\pi \ln(m_Z/\mu)]^n$ also enter, for example, in the relation between $\sin^2\theta_W$ at the scales m_Z (LEP, SLC) and μ (e.g. the scale of low-energy neutral-current experiments). Also, large logs from initial state radiation dramatically distort the line shape of the Z resonance as observed at LEP1 and SLC and this effect was accurately taken into account for the measurement of the Z mass and total width. The experimental accuracy on m_Z obtained at LEP1 is $\delta m_Z = \pm 2.1$ MeV (see Chap. 6). Similarly, a measurement of the total width to an accuracy $\delta\Gamma = \pm 2.3$ MeV has been achieved. The prediction of the Z line-shape in the SM to such an accuracy has posed a formidable challenge to theory, which has been successfully met. For the inclusive process $e^+e^- \rightarrow f\bar{f}X$, with $f \neq e$ (for a concise discussion, we leave Bhabha scattering aside) and X including γ 's and gluons, the physical cross-section can be written in the form of a convolution [42]:

$$\sigma(s) = \int_{z_0}^1 dz \hat{\sigma}(zs)G(z, s), \quad (3.95)$$

where $\hat{\sigma}$ is the reduced cross-section, and $G(z, s)$ is the radiator function that describes the effect of initial-state radiation; $\hat{\sigma}$ includes the purely weak corrections, the effect of final-state radiation (of both γ 's and gluons), and also non-factorizable terms (initial- and final-state radiation interferences, boxes, etc.) which, being small, can be treated in lowest order and effectively absorbed in a modified $\hat{\sigma}$. The radiator $G(z, s)$ has an expansion of the form

$$G(z, s) = \delta(1-z) + \alpha/\pi(a_{11}L + a_{10}) + (\alpha/\pi)^2(a_{22}L^2 + a_{11}L + a_{20}) + \dots + (\alpha/\pi)^n \sum_{i=0}^n a_{ni}L^i, \quad (3.96)$$

where $L = \ln s/m_e^2 \simeq 24.2$ for $\sqrt{s} \simeq m_Z$. All first- and second-order terms are known exactly. The sequence of leading and next-to-leading logs can be exponentiated (closely following the formalism of structure functions in QCD). For $m_Z \approx 91$ GeV, the convolution displaces the peak by +110 MeV, and reduces it by a factor of about 0.74. The exponentiation is important in that it amounts to an additional shift of about 14 MeV in the peak position with respect to the one loop radiative correction.

Among the one loop EW radiative corrections, a very remarkable class of contributions are those terms that increase quadratically with the top mass. The sensitivity of radiative corrections to m_t arises from the existence of these terms. The

quadratic dependence on m_t (and on other possible widely broken isospin multiplets from new physics) arises because, in spontaneously broken gauge theories, heavy virtual particles do not decouple. On the contrary, in QED or QCD, the running of α and α_s at a scale Q is not affected by heavy quarks with mass $M \gg Q$. According to an intuitive decoupling theorem [43], diagrams with heavy virtual particles of mass M can be ignored at $Q \ll M$ provided that the couplings do not grow with M and that the theory with no heavy particles is still renormalizable. In the spontaneously broken EW gauge theories both requirements are violated. First, one important difference with respect to unbroken gauge theories is in the longitudinal modes of weak gauge bosons. These modes are generated by the Higgs mechanism, and their couplings grow with masses (as is also the case for the physical Higgs couplings). Second the theory without the top quark is no more renormalizable because the gauge symmetry is broken as the (t,b) doublet would not be complete (also the chiral anomaly would not be completely cancelled). With the observed value of m_t the quantitative importance of the terms of order $G_F m_t^2 / 4\pi^2 \sqrt{2}$ is substantial but not dominant (they are enhanced by a factor $m_t^2 / m_W^2 \sim 5$ with respect to ordinary terms). Both the large logarithms and the $G_F m_t^2$ terms have a simple structure and are to a large extent universal, i.e. common to a wide class of processes. In particular the $G_F m_t^2$ terms appear in vacuum polarization diagrams which are universal (virtual loops inserted in gauge boson internal lines are independent of the nature of the vertices on each side of the propagator) and in the $Z \rightarrow b\bar{b}$ vertex which is not. This vertex is specifically sensitive to the top quark which, being the partner of the b quark in a doublet, runs in the loop. Instead all types of heavy particles could in principle contribute to vacuum polarization diagrams. The study of universal vacuum polarization contributions, also called “oblique” corrections, and of top enhanced terms is important for an understanding of the pattern of radiative corrections. More in general, the important consequence of non decoupling is that precision tests of the electroweak theory may a priori be sensitive to new physics even if the new particles are too heavy for their direct production, but a posteriori no signal of deviation has clearly emerged.

While radiative corrections are quite sensitive to the top mass, they are unfortunately much less dependent on the Higgs mass. If they were sufficiently sensitive by now we would precisely know the mass of the Higgs. But the dependence of one loop diagrams on m_H is only logarithmic: $\sim G_F m_W^2 \log(m_H^2 / m_W^2)$. Quadratic terms $\sim G_F^2 m_H^2$ only appear at two loops [44] and are too small to be detectable. The difference with the top case is that the splitting $m_t^2 - m_b^2$ is a direct breaking of the gauge symmetry that already affects the 1-loop corrections, while the Higgs couplings are “custodial” SU(2) symmetric in lowest order.

3.11 Electroweak Precision Tests in the SM and Beyond

For the analysis of electroweak data in the SM one starts from the input parameters: as is the case in any renormalizable theory, masses and couplings have to be specified from outside. One can trade one parameter for another and this freedom is used to select the best measured ones as input parameters. Some of them, α , G_F and m_Z , are very precisely known, as we have seen, some other ones, m_{light} , m_t and $\alpha_s(m_Z)$ are less well determined while m_H is largely unknown. Among the light fermions, the quark masses are badly known, but fortunately, for the calculation of radiative corrections, they can be replaced by $\alpha(m_Z)$, the value of the QED running coupling at the Z mass scale. The value of the hadronic contribution to the running, embodied in the value of $\Delta\alpha_{\text{had}}^{(5)}(m_Z^2)$ (see Table 3.1, [8]) is obtained through dispersion relations from the data on $e^+e^- \rightarrow \text{hadrons}$ at moderate centre-of-mass energies. From the input parameters one computes the radiative corrections to a sufficient precision to match the experimental accuracy. Then one compares the theoretical predictions with the data for the numerous observables which have been measured [45], checks the consistency of the theory and derives constraints on m_t , $\alpha_s(m_Z)$ and m_H . A detailed discussion of all experimental aspects of precision tests of the EW theory is presented in Chap. 6.

The basic tree level relations:

$$\frac{g^2}{8m_W^2} = \frac{G_F}{\sqrt{2}}, \quad g^2 \sin^2 \theta_W = e^2 = 4\pi\alpha \quad (3.97)$$

can be combined into

$$\sin^2 \theta_W = \frac{\pi\alpha}{\sqrt{2}G_F m_W^2} \quad (3.98)$$

Always at tree level, a different definition of $\sin^2 \theta_W$ is from the gauge boson masses:

$$\frac{m_W^2}{m_Z^2 \cos^2 \theta_W} = \rho_0 = 1 \quad \Longrightarrow \quad \sin^2 \theta_W = 1 - \frac{m_W^2}{m_Z^2} \quad (3.99)$$

where $\rho_0 = 1$ assuming that there are only Higgs doublets. The last two relations can be put into the convenient form

$$\left(1 - \frac{m_W^2}{m_Z^2}\right) \frac{m_W^2}{m_Z^2} = \frac{\pi\alpha}{\sqrt{2}G_F m_Z^2} \quad (3.100)$$

Beyond tree level, these relations are modified by radiative corrections:

$$\begin{aligned} \left(1 - \frac{m_W^2}{m_Z^2}\right) \frac{m_W^2}{m_Z^2} &= \frac{\pi\alpha(m_Z)}{\sqrt{2}G_F m_Z^2} \frac{1}{1 - \Delta r_W} \\ \frac{m_W^2}{m_Z^2 \cos^2 \theta_W} &= 1 + \Delta\rho_m \end{aligned} \quad (3.101)$$

The Z and W masses are to be precisely defined in terms of the pole position in the respective propagators. Then, in the first relation the replacement of α with the running coupling at the Z mass $\alpha(m_Z)$ makes Δr_W completely determined at 1-loop by purely weak corrections (G_F is protected from logarithmic running as an indirect consequence of (V-A) current conservation in the massless theory). This relation defines Δr_W unambiguously, once the meaning of $\alpha(m_Z)$ is specified (for example, \overline{MS}). On the contrary, in the second relation $\Delta\rho_m$ depends on the definition of $\sin^2 \theta_W$ beyond the tree level. For LEP physics $\sin^2 \theta_W$ is usually defined from the $Z \rightarrow \mu^+ \mu^-$ effective vertex. At the tree level the vector and axial-vector couplings g_V^μ and g_A^μ are given in Eqs. (3.29). Beyond the tree level a corrected vertex can be written down in terms of modified effective couplings. Then $\sin^2 \theta_W \equiv \sin^2 \theta_{eff}$ is in general defined through the muon vertex:

$$\begin{aligned} g_V^\mu / g_A^\mu &= 1 - 4 \sin^2 \theta_{eff} \\ \sin^2 \theta_{eff} &= (1 + \Delta k) s_0^2, \quad s_0^2 c_0^2 = \frac{\pi\alpha(m_Z)}{\sqrt{2}G_F m_Z^2} \\ g_A^{\mu 2} &= \frac{1}{4}(1 + \Delta\rho) \end{aligned} \quad (3.102)$$

We see that s_0^2 and c_0^2 are ‘‘improved’’ Born approximations (by including the running of α) for $\sin^2 \theta_{eff}$ and $\cos^2 \theta_{eff}$. Actually, since in the SM lepton universality is only broken by masses and is in agreement with experiment within the present accuracy, in practice the muon channel can be replaced with the average over charged leptons.

We can write a symbolic equation that summarizes the status of what has been computed up to now for the radiative corrections (we list some recent work on each item from where older references can be retrieved) Δr_W [46], $\Delta\rho$ [47] and Δk [48]:

$$\Delta r_W, \Delta\rho, \Delta k = g^2 \frac{m_t^2}{m_W^2} (1 + \alpha_s + \alpha_s^2) + g^2 (1 + \alpha_s + \sim \alpha_s^2) + g^4 \frac{m_t^4}{m_W^4} + g^4 \frac{m_t^2}{m_W^2} + \dots \quad (3.103)$$

The meaning of this relation is that the one loop terms of order g^2 are completely known, together with their first order QCD corrections (the second order QCD

corrections are only estimated for the g^2 terms not enhanced by m_t^2/m_W^2 , and the terms of order g^4 enhanced by the ratios m_t^4/m_W^4 or m_t^2/m_W^2 are also known.

In the SM the quantities Δr_W , $\Delta\rho$, Δk , for sufficiently large m_t , are all dominated by quadratic terms in m_t of order $G_F m_t^2$. The quantity $\Delta\rho_m$ is not independent and can be expressed in terms of them. As new physics can more easily be disentangled if not masked by large conventional m_t effects, it is convenient to keep $\Delta\rho$ while trading Δr_W and Δk for two quantities with no contributions of order $G_F m_t^2$. One thus introduces the following linear combinations (epsilon parameters) [49]:

$$\begin{aligned}\epsilon_1 &= \Delta\rho, \\ \epsilon_2 &= c_0^2 \Delta\rho + \frac{s_0^2 \Delta r_W}{c_0^2 - s_0^2} - 2s_0^2 \Delta k, \\ \epsilon_3 &= c_0^2 \Delta\rho + (c_0^2 - s_0^2) \Delta k.\end{aligned}\tag{3.104}$$

The quantities ϵ_2 and ϵ_3 no longer contain terms of order $G_F m_t^2$ but only logarithmic terms in m_t . The leading terms for large Higgs mass, which are logarithmic, are contained in ϵ_1 and ϵ_3 . To complete the set of top-enhanced radiative corrections one adds ϵ_b defined from the loop corrections to the $Zb\bar{b}$ vertex. One modifies g_V^b and g_A^b as follows:

$$\begin{aligned}g_A^b &= -\frac{1}{2}\left(1 + \frac{\Delta\rho}{2}\right)(1 + \epsilon_b), \\ \frac{g_V^b}{g_A^b} &= \frac{1 - 4/3 \sin^2 \theta_{eff} + \epsilon_b}{1 + \epsilon_b}.\end{aligned}\tag{3.105}$$

ϵ_b can be measured from $R_b = \Gamma(Z \rightarrow b\bar{b})/\Gamma(Z \rightarrow \text{hadrons})$ (see Table 3.1). This is clearly not the most general deviation from the SM in the $Z \rightarrow b\bar{b}$ vertex but ϵ_b is the quantity where the large m_t corrections are located in the SM. Thus, summarizing, in the SM one has the following ‘‘large’’ asymptotic contributions:

$$\begin{aligned}\epsilon_1 &= \frac{3G_F m_t^2}{8\pi^2 \sqrt{2}} - \frac{3G_F m_W^2}{4\pi^2 \sqrt{2}} \tan^2 \theta_W \ln \frac{m_H}{m_Z} + \dots, \\ \epsilon_2 &= -\frac{G_F m_W^2}{2\pi^2 \sqrt{2}} \ln \frac{m_t}{m_Z} + \dots, \\ \epsilon_3 &= \frac{G_F m_W^2}{12\pi^2 \sqrt{2}} \ln \frac{m_H}{m_Z} - \frac{G_F m_W^2}{6\pi^2 \sqrt{2}} \ln \frac{m_t}{m_Z} \dots, \\ \epsilon_b &= -\frac{G_F m_t^2}{4\pi^2 \sqrt{2}} + \dots\end{aligned}\tag{3.106}$$

The ϵ_i parameters vanish in the limit where only tree level SM effects are kept plus pure QED and/or QCD corrections. So they describe the effects of quantum corrections (i.e. loops) from weak interactions. A similar set of parameters are the S, T, U parameters [50]: the shifts induced by new physics on S, T and U are proportional to those induced on ϵ_3 , ϵ_1 and ϵ_2 , respectively. In principle, with no model dependence, one can measure the four ϵ_i from the basic observables of LEP physics $\Gamma(Z \rightarrow \mu^+\mu^-)$, A_{FB}^μ and R_b on the Z peak plus m_W . With increasing model dependence, one can include other measurements in the fit for the ϵ_i . For example, use lepton universality to average the μ with the e and τ final states, or include all lepton asymmetries and so on. The present experimental values of the ϵ_i , obtained from a fit of all LEP1-SLD measurements plus m_W , are given by The LEP Electroweak Working Group [8]:

$$\begin{aligned}\epsilon_1 \cdot 10^3 &= 5.4 \pm 1.0, & \epsilon_2 \cdot 10^3 &= -8.9 \pm 1.2, \\ \epsilon_3 \cdot 10^3 &= 5.34 \pm 0.94, & \epsilon_b \cdot 10^3 &= -5.0 \pm 1.6.\end{aligned}\quad (3.107)$$

Note that the ϵ parameters are of order a few in 10^{-3} and are known with an accuracy in the range 15–30%. As discussed in the next Section, these values are in agreement with the SM with a light Higgs. All models of new physics must be compared with these findings and pass this difficult test.

3.12 Results of the SM Analysis of Precision Tests

The electroweak Z pole measurements, combining the results of all the experiments, are summarised in Table 3.1. The various asymmetries determine the effective electroweak mixing angle for leptons with highest sensitivity. The weighted average of these results, including small correlations, is:

$$\sin^2 \theta_{eff} = 0.23153 \pm 0.00016, \quad (3.108)$$

Note, however, that this average has a χ^2 of 11.8 for 5 degrees of freedom, corresponding to a probability of a few %. The χ^2 is pushed up by the two most precise measurements of $\sin^2 \theta_{eff}$, namely those derived from the measurements of A_l by SLD, dominated by the left-right asymmetry A_{LR}^0 , and of the forward-backward asymmetry measured in $b\bar{b}$ production at LEP, $A_{FB}^{0,b}$, which differ by about 3σ .

We now discuss fitting the data in the SM. One can think of different types of fit, depending on which experimental results are included or which answers one wants to obtain. For example, in Table 3.2 we present in column 1 a fit of all Z pole data plus m_W and Γ_W (this is interesting as it shows the value of m_t obtained indirectly from radiative corrections, to be compared with the value of m_t measured in production experiments), in column 2 a fit of all Z pole data plus

Table 3.1 Summary of electroweak precision measurements at high Q^2 [8]

Observable	Measurement	SM fit
m_Z [GeV]	91.1875 ± 0.0021	91.1875
Γ_Z [GeV]	2.4952 ± 0.0023	2.4957
σ_h^0 [nb]	41.540 ± 0.037	41.477
R_l^0	20.767 ± 0.025	20.744
$AFB^{0,l}$	0.01714 ± 0.00095	0.01645
A_l (SLD)	0.1513 ± 0.0021	0.1481
A_l (P_τ)	0.1465 ± 0.0032	0.1481
R_b^0	0.21629 ± 0.00066	0.21586
R_c^0	0.1721 ± 0.0030	0.1722
$A_{FB}^{0,b}$	0.0992 ± 0.0016	0.1038
$A_{FB}^{0,c}$	0.0707 ± 0.0035	0.0742
A_b	0.923 ± 0.020	0.935
A_c	0.670 ± 0.027	0.668
$\sin^2 \theta_{eff} (Q_{FB}^{had})$	0.2324 ± 0.0012	0.2314
m_W [GeV]	80.398 ± 0.025	80.374
Γ_W [GeV]	2.140 ± 0.060	2.091
m_t [GeV] ($p\bar{p}$)	170.9 ± 1.8	171.3
$\Delta\alpha_{had}^{(5)}(m_Z^2)$	0.02758 ± 0.00035	0.02768

The first block shows the Z-pole measurements. The second block shows additional results from other experiments: the mass and the width of the W boson measured at the Tevatron and at LEP-2, the mass of the top quark measured at the Tevatron, and the contribution to α of the hadronic vacuum polarization. The SM fit results are derived from the SM analysis of these results

m_t (here it is m_W which is indirectly determined), and, finally, in column 3 a fit of all the data listed in Table 3.1 (which is the most relevant fit for constraining m_H). From the fit in column 1 of Table 3.2 we see that the extracted value of m_t is in good agreement with the direct measurement (see Table 3.1). Similarly we see that the experimental measurement of m_W in Table 3.1 is larger by about one standard deviation with respect to the value from the fit in column 2. We have seen that quantum corrections depend only logarithmically on m_H . In spite of this small sensitivity, the measurements are precise enough that one still obtains a quantitative indication of the mass range. From the fit in column 3 we obtain: $\log_{10} m_H(\text{GeV}) = 1.88 \pm 0.16$ (or $m_H = 76_{-24}^{+34}$ GeV). This result on the Higgs mass is particularly remarkable. The value of $\log_{10} m_H(\text{GeV})$ is compatible with the small window between ~ 2 and ~ 3 which is allowed, on the one side, by the direct search limit ($m_H > 114$ GeV from LEP-2 [8]), and, on the other side, by the theoretical upper limit on the Higgs mass in the minimal SM, $m_H \lesssim 600 - 800$ GeV [51].

Thus the whole picture of a perturbative theory with a fundamental Higgs is well supported by the data on radiative corrections. It is important that there is a clear indication for a particularly light Higgs: at 95% c.l. $m_H \lesssim 182$ GeV (including

Table 3.2 Standard Model fits of electroweak data [8]

Fit	1	2	3
Measurements	m_W	m_t	m_t, m_W
m_t (GeV)	178.9^{+12}_-9	170.9 ± 1.8	171.3 ± 1.7
m_H (GeV)	145^{+240}_{-81}	99^{+52}_{-35}	76^{+34}_{-24}
$\log [m_H \text{ (GeV)}]$	2.16 ± 0.39	2.00 ± 0.19	1.88 ± 0.16
$\alpha_s(m_Z)$	0.1190 ± 0.0028	0.1189 ± 0.0027	0.1185 ± 0.0026
m_W (MeV)	80385 ± 19	80360 ± 20	80374 ± 15

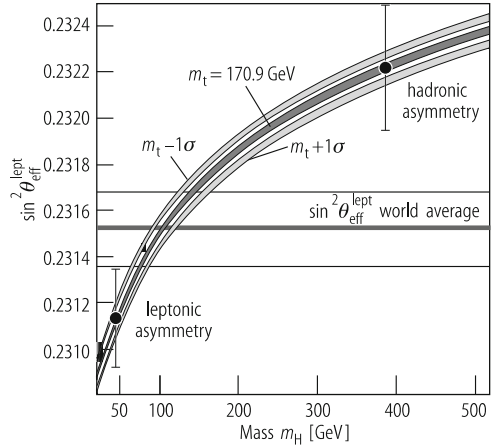
All fits use the Z pole results and $\Delta\alpha_{had}^{(5)}(m_Z^2)$ as listed in Table 3.1. In addition, the measurements listed on top of each column are included as well. The fitted W mass is also shown [8] (the directly measured value is $m_W = 80398 \pm 25$ MeV)

the input from the direct search result). This is quite encouraging for the ongoing search for the Higgs particle. More general, if the Higgs couplings are removed from the Lagrangian the resulting theory is non renormalizable. A cutoff Λ must be introduced. In the quantum corrections $\log m_H$ is then replaced by $\log \Lambda$ plus a constant. The precise determination of the associated finite terms would be lost (that is, the value of the mass in the denominator in the argument of the logarithm). A heavy Higgs would need some unfortunate accident: the finite terms, different in the new theory from those of the SM, should by chance compensate for the heavy Higgs in a few key parameters of the radiative corrections (mainly ϵ_1 and ϵ_3 , see, for example, [49]). Alternatively, additional new physics, for example in the form of effective contact terms added to the minimal SM lagrangian, should accidentally do the compensation, which again needs some sort of conspiracy.

To the list of precision tests of the SM one should add the results on low energy tests obtained from neutrino and antineutrino deep inelastic scattering (NuTeV [52]), parity violation in Cs atoms (APV [53]) and the recent measurement of the parity-violating asymmetry in Moller scattering [54] (see Chap. 6). When these experimental results are compared with the SM predictions the agreement is good except for the NuTeV result that shows a deviation by three standard deviations. The NuTeV measurement is quoted as a measurement of $\sin^2 \theta_W = 1 - m_W^2/m_Z^2$ from the ratio of neutral to charged current deep inelastic cross-sections from ν_μ and $\bar{\nu}_\mu$ using the Fermilab beams. But it has been argued and it is now generally accepted that the NuTeV anomaly probably simply arises from an underestimation of the theoretical uncertainty in the QCD analysis needed to extract $\sin^2 \theta_W$. In fact, the lowest order QCD parton formalism on which the analysis has been based is too crude to match the experimental accuracy.

When confronted with these results, on the whole the SM performs rather well, so that it is fair to say that no clear indication for new physics emerges from the data. However, as already mentioned, one problem is that the two most precise measurements of $\sin^2 \theta_{eff}$ from A_{LR} and A_{FB}^b differ by about 3σ s. In general, there appears to be a discrepancy between $\sin^2 \theta_{eff}$ measured from leptonic asymmetries ($(\sin^2 \theta_{eff})_l$) and from hadronic asymmetries ($(\sin^2 \theta_{eff})_h$). In fact, the result from

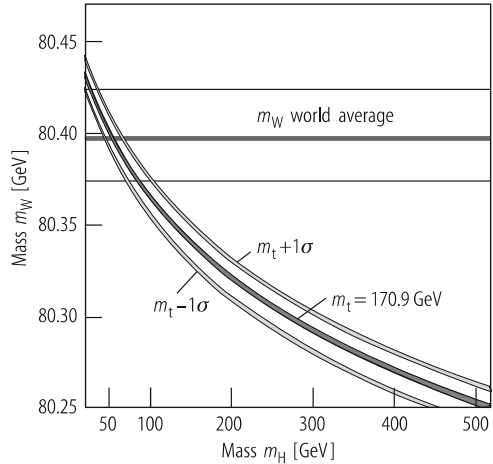
Fig. 3.11 The data for $\sin^2 \theta_{\text{eff}}^{\text{lept}}$ are plotted vs m_H . The theoretical prediction for the measured value of m_t is also shown. For presentation purposes the measured points are shown each at the m_H value that would ideally correspond to it given the central value of m_t (updated from [55])



A_{LR} is in good agreement with the leptonic asymmetries measured at LEP, while all hadronic asymmetries, though their errors are large, are better compatible with the result of A_{FB}^b . These two results for $\sin^2 \theta_{\text{eff}}$ are shown in Fig. 3.11 [55]. Each of them is plotted at the m_H value that would correspond to it given the central value of m_t . Of course, the value for m_H indicated by each $\sin^2 \theta_{\text{eff}}$ has an horizontal ambiguity determined by the measurement error and the width of the $\pm 1\sigma$ band for m_t . Even taking this spread into account it is clear that the implications on m_H are sizably different. One might imagine that some new physics effect could be hidden in the $Zb\bar{b}$ vertex. Like for the top quark mass there could be other non decoupling effects from new heavy states or a mixing of the b quark with some other heavy quark. However, it is well known that this discrepancy is not easily explained in terms of some new physics effect in the $Zb\bar{b}$ vertex. A rather large change with respect to the SM of the b-quark right handed coupling to the Z is needed in order to reproduce the measured discrepancy (precisely a $\sim 30\%$ change in the right-handed coupling), an effect too large to be a loop effect but which could be produced at the tree level, e.g., by mixing of the b quark with a new heavy vectorlike quark [56]), or some mixing of the Z with ad hoc heavy states [57]. But then this effect should normally also appear in the direct measurement of A_b performed at SLD using the left-right polarized b asymmetry, even within the moderate precision of this result. The measurements of neither A_b at SLD nor R_b confirm the need of a new effect. Alternatively, the observed discrepancy could be simply due to a large statistical fluctuation or an unknown experimental problem. As a consequence of this problem, the ambiguity in the measured value of $\sin^2 \theta_{\text{eff}}$ is in practice larger than the nominal error, reported in Eq. 3.108, obtained from averaging all the existing determinations, and the interpretation of precision tests is less sharp than it would otherwise be.

We have already observed that the experimental value of m_W (with good agreement between LEP and the Tevatron) is a bit high compared to the SM prediction (see Fig. 3.12). The value of m_H indicated by m_W is on the low side, just in the same interval as for $\sin^2 \theta_{\text{eff}}^{\text{lept}}$ measured from leptonic asymmetries.

Fig. 3.12 The data for m_W are plotted vs m_H . The theoretical prediction for the measured value of m_t is also shown (updated from [55])



In conclusion, overall the validity of the SM has been confirmed to a level that we can say was unexpected at the beginning. In the present data there is no significant evidence for departures from the SM, no compelling evidence of new physics. The impressive success of the SM poses strong limitations on the possible forms of new physics.

3.13 Phenomenology of the SM Higgs

The Higgs problem is really central in particle physics today. On the one hand, the experimental verification of the Standard Model (SM) cannot be considered complete until the structure of the Higgs sector is not established by experiment. On the other hand, the Higgs is also related to most of the major problems of particle physics, like the flavour problem and the hierarchy problem, the latter strongly suggesting the need for new physics near the weak scale. In turn the discovery of new physics could clarify the dark matter identity. It is clear that the fact that some sort of Higgs mechanism is at work has already been established. The W or the Z with longitudinal polarization that we observe are not present in an unbroken gauge theory (massless spin-1 particles, like the photon, are transversely polarized). The longitudinal degree of freedom for the W or the Z is borrowed from the Higgs sector and is an evidence for it. Also, it has been verified that the gauge symmetry is unbroken in the vertices of the theory: all currents and charges are indeed symmetric. Yet there is obvious evidence that the symmetry is instead badly broken in the masses. Not only the W and the Z have large masses, but the large splitting of, for example, the t-b doublet shows that even a global weak SU(2) is not at all respected by the fermion spectrum. This is a clear signal of spontaneous symmetry breaking and the implementation of spontaneous symmetry breaking in a

gauge theory is via the Higgs mechanism. The big remaining questions are about the nature and the properties of the Higgs particle(s). The present experimental information on the Higgs sector, is surprisingly limited and can be summarized in a few lines, as follows. First, the relation $M_W^2 = M_Z^2 \cos^2 \theta_W$, Eq. (3.55), modified by small, computable radiative corrections, has been experimentally proven. This relation means that the effective Higgs (be it fundamental or composite) is indeed a weak isospin doublet. The Higgs particle has not been found but, in the SM, its mass can well be larger than the present direct lower limit $m_H \gtrsim 114 \text{ GeV}$ (at 95% c.l.) obtained from searches at LEP-2. The radiative corrections computed in the SM when compared to the data on precision electroweak tests lead to a clear indication for a light Higgs, not too far from the present lower bound. The exact experimental upper limit for m_H in the SM depends on the value of the top quark mass m_t . The CDF and D0 combined value after Run II is at present [8] $m_t = 170.9 \pm 1.8 \text{ GeV}$ (it went down with respect to the value $m_t = 178 \pm 4.3 \text{ GeV}$ from Run I and also the experimental error is now sizably reduced). As a consequence the present limit on m_H is more stringent [8]: $m_H < 182 \text{ GeV}$ (at 95% c.l., after including the information from the 114 GeV direct bound). On the Higgs the LHC will address the following questions : one doublet, more doublets, additional singlets? SM Higgs or SUSY Higgses? Fundamental or composite (of fermions, of WW...)? Pseudo-Goldstone boson of an enlarged symmetry? A manifestation of large extra dimensions (5th component of a gauge boson, an effect of orbifolding or of boundary conditions...)? Or some combination of the above or something so far unthought of? Here in the following we will summarize the main properties of the SM Higgs that provide an essential basis for the planning and the interpretation of the LHC Higgs programme. We start from the mass, then the width and the branching ratios and, finally, the most important production channels.

3.13.1 Theoretical Bounds on the SM Higgs Mass

It is well known [58–60] that in the SM with only one Higgs doublet a lower limit on m_H can be derived from the requirement of vacuum stability (or, in milder form, of a moderate instability, compatible with the lifetime of the Universe [61]). The limit is a function of m_t and of the energy scale Λ where the model breaks down and new physics appears. The Higgs mass enters because it fixes the initial value of the quartic Higgs coupling λ for its running up to the large scale Λ . Similarly an upper bound on m_H (with mild dependence on m_t) is obtained, as described in [62] and refs. therein, from the requirement that for λ no Landau pole appears up to the scale Λ , or in simpler terms, that the perturbative description of the theory remains valid up to Λ . We now briefly recall the derivation of these limits.

The possible instability of the Higgs potential $V[\phi]$ is generated by the quantum loop corrections to the classical expression of $V[\phi]$. At large ϕ the derivative

$V'[\phi]$ could become negative and the potential would become unbound from below. The one-loop corrections to $V[\phi]$ in the SM are well known and change the dominant term at large ϕ according to $\lambda\phi^4 \rightarrow (\lambda + \gamma \log \phi^2/\Lambda^2)\phi^4$. This one-loop approximation is not enough in this case, because it fails at large enough ϕ , when $\gamma \log \phi^2/\Lambda^2$ becomes of order one. The renormalization group improved version of the corrected potential leads to the replacement $\lambda\phi^4 \rightarrow \lambda(\Lambda)\phi'^4(\Lambda)$ where $\lambda(\Lambda)$ is the running coupling and $\phi'(\mu) = \phi \exp \int^t \gamma(t') dt'$, with $\gamma(t)$ being an anomalous dimension function and $t = \log \Lambda/v$ (v is the vacuum expectation value $v = (2\sqrt{2}G_F)^{-1/2}$). As a result, the positivity condition for the potential amounts to the requirement that the running coupling $\lambda(\Lambda)$ never becomes negative. A more precise calculation, which also takes into account the quadratic term in the potential, confirms that the requirements of positive $\lambda(\Lambda)$ leads to the correct bound down to scales Λ as low as ~ 1 TeV. The running of $\lambda(\Lambda)$ at one loop is given by:

$$\frac{d\lambda}{dt} = \frac{3}{4\pi^2} [\lambda^2 + 3\lambda h_t^2 - 9h_t^4 + \text{small gauge and Yukawa terms}], \quad (3.109)$$

with the normalization such that at $t = 0$, $\lambda = \lambda_0 = m_H^2/2v^2$ and the top Yukawa coupling $h_t^0 = m_t/v$. We see that, for m_H small and m_t fixed at its measured value, λ decreases with t and can become negative. If one requires that λ remains positive up to $\Lambda = 10^{15} - 10^{19}$ GeV, then the resulting bound on m_H in the SM with only one Higgs doublet is given by, (also including the effect of the two-loop beta function terms) [60]:

$$m_H (\text{GeV}) > 128.4 + 2.1 [m_t - 170.9] - 4.5 \frac{\alpha_s(m_Z) - 0.118}{0.006}. \quad (3.110)$$

Note that this limit is evaded in models with more Higgs doublets. In this case the limit applies to some average mass but the lightest Higgs particle can well be below, as it is the case in the minimal SUSY extension of the SM (MSSM).

The upper limit on the Higgs mass in the SM is clearly important for assessing the chances of success of the LHC as an accelerator designed to solve the Higgs problem. The upper limit [62] arises from the requirement that the Landau pole associated with the non asymptotically free behaviour of the $\lambda\phi^4$ theory does not occur below the scale Λ . The initial value of λ at the weak scale increases with m_H and the derivative is positive at large λ (because of the positive λ^2 term—the $\lambda\phi^4$ theory is not asymptotically free—which overwhelms the negative top-Yukawa term). Thus, if m_H is too large, the point where λ computed from the perturbative beta function becomes infinite (the Landau pole) occurs at too low an energy. Of course in the vicinity of the Landau pole the 2-loop evaluation of the beta function is not reliable. Indeed the limit indicates the frontier of the domain where the theory is well described by the perturbative expansion. Thus the quantitative evaluation of the limit is only indicative, although it has been to some extent supported by simulations of the Higgs sector of the EW theory on the lattice. For the upper limit

on m_H one finds [62]

$$\begin{aligned} m_H &\lesssim 180 \text{ GeV for } \Lambda \sim M_{GUT} - M_{Pl} \\ m_H &\lesssim 0.5 - 0.8 \text{ TeV for } \Lambda \sim 1 \text{ TeV}. \end{aligned} \quad (3.111)$$

In conclusion, for $m_t \sim 171 \text{ GeV}$, only a small range of values for m_H is allowed, $130 < m_H < \sim 200 \text{ GeV}$, if the SM holds up to $\Lambda \sim M_{GUT}$ or M_{Pl} .

An additional argument indicating that the solution of the Higgs problem cannot be too far away is the fact that, in the absence of a Higgs particle or of an alternative mechanism, violations of unitarity appear in some scattering amplitudes at energies in the few TeV range [63]. In particular, amplitudes involving longitudinal gauge bosons (those most directly related to the Higgs sector) are affected. For example, at tree level in the absence of Higgs exchange, for $s \gg m_Z^2$ one obtains:

$$A(W_L^+ W_L^- \rightarrow Z_L Z_L)_{no \text{ Higgs}} \sim i \frac{s}{v^2} \quad (3.112)$$

In the SM this unacceptable large energy behaviour is quenched by the Higgs exchange diagram contribution:

$$A(W_L^+ W_L^- \rightarrow Z_L Z_L)_{Higgs} \sim -i \frac{s^2}{v^2(s - m_H^2)} \quad (3.113)$$

Thus the total result in the SM is:

$$A(W_L^+ W_L^- \rightarrow Z_L Z_L)_{SM} \sim -i \frac{sm_H^2}{v^2(s - m_H^2)} \quad (3.114)$$

which at large energies saturates at a constant value. To be compatible with unitarity bounds one needs $m_H^2 < 4\pi\sqrt{2}/G_F$ or $m_H < 1.5 \text{ TeV}$. Both the Landau pole and the unitarity argument show that, if the Higgs is too heavy, the SM becomes a non perturbative theory at energies of $\mathcal{O}(1 \text{ TeV})$. In conclusion, these arguments imply that the SM Higgs cannot escape detection at the LHC.

3.13.2 SM Higgs Decays

The total width and the branching ratios for the SM Higgs as function of m_H are given in Figs. 3.13 and 3.14, respectively [64].

Since the couplings of the Higgs particle are in proportion to masses, when m_H increases the Higgs becomes strongly coupled. This is reflected in the sharp rise of the total width with m_H . For m_H near its present lower bound of 114 GeV , the width is below 5 MeV , much less than for the W or the Z which have a comparable mass.

Fig. 3.13 The total width of the SM Higgs boson [64]

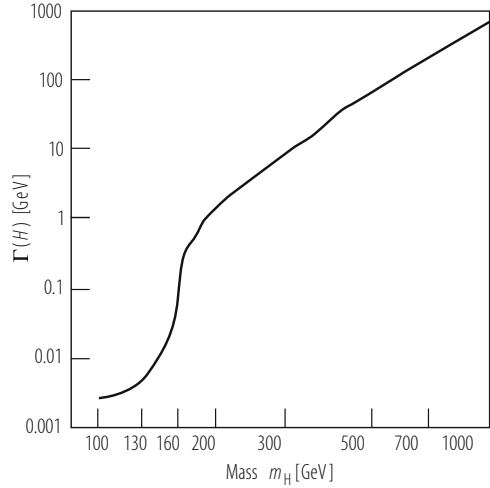
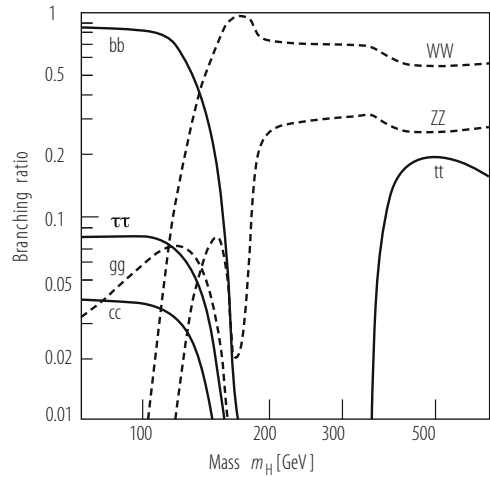


Fig. 3.14 The branching ratios of the SM Higgs boson [65]



The dominant channel for such a Higgs is $H \rightarrow b\bar{b}$. In Born approximation the partial width into a fermion pair is given by Djouadi [64] and Haber [66]:

$$\Gamma(H \rightarrow f\bar{f}) = N_C \frac{G_F}{4\pi\sqrt{2}} m_H m_f^2 \beta_f^3 \quad (3.115)$$

where $\beta_f = (1 - 4m_f^2/m_H^2)^{1/2}$. The factor of β^3 appears because the fermion pair must be in a p-state of orbital angular momentum for a Higgs with scalar coupling, because of parity (this factor would be β for a pseudoscalar coupling). We see that the width is suppressed by a factor m_f^2/m_H^2 with respect to the natural size $G_F m_H^3$

for the width of a particle of mass m_H decaying through a diagram with only one weak vertex.

A glance to the branching ratios shows that the branching ratio into τ pairs is larger by more than a factor of two with respect to the $c\bar{c}$ channel. This is at first sight surprising because the colour factor N_C favours the quark channels and the masses of τ 's and of D mesons are quite similar. This is due to the fact that the QCD corrections replace the charm mass at the scale of charm with the charm mass at the scale m_H , which is lower by about a factor of 2.5. The masses run logarithmically in QCD, similar to the coupling constant. The corresponding logs are already present in the 1-loop QCD correction that amounts to the replacement $m_q^2 \rightarrow m_q^2[1 + 2\alpha_s/\pi(\log m_q^2/m_H^2 + 3/2)] \sim m_q^2(m_H^2)$.

The Higgs width sharply increases as the WW threshold is approached. For decay into a real pair of V 's, with $V = W, Z$, one obtains in Born approximation [64, 66]:

$$\Gamma(H \rightarrow VV) = \frac{G_F m_H^3}{16\pi\sqrt{2}} \delta_V \beta_W (1 - 4x + 12x^2) \quad (3.116)$$

where $\beta_W = \sqrt{1 - 4x}$ with $x = m_V^2/m_H^2$ and $\delta_W = 2$, $\delta_Z = 1$. Much above threshold the VV channels are dominant and the total width, given approximately by:

$$\Gamma_H \sim 0.5 \text{ TeV} \left(\frac{m_H}{1 \text{ TeV}}\right)^3 \quad (3.117)$$

becomes very large, signalling that the Higgs sector is becoming strongly interacting (recall the upper limit on the SM Higgs mass in Eq. (3.111)). The VV dominates over the $t\bar{t}$ because of the β threshold factors that disfavour the fermion channel and, at large m_H , by the cubic versus linear behaviour with m_H of the partial widths for VV versus $t\bar{t}$. Below the VV threshold the decays into virtual V particles is important: VV^* and V^*V^* . Note in particular the dip of the ZZ branching ratio just below the ZZ threshold: this is due to the fact that the W is lighter than the Z and the opening of its threshold depletes all other branching ratios. When the ZZ threshold is also passed then the ZZ branching fraction comes back to the ratio of approximately 1:2 with the WW channel (just the number of degrees of freedom: two hermitian fields for the W , one for the Z).

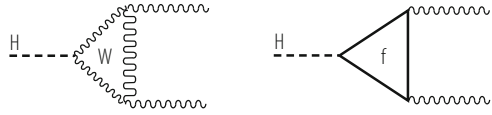
The decay channels into $\gamma\gamma$, $Z\gamma$ and gg proceed through loop diagrams, with the contributions from W (only for $\gamma\gamma$ and $Z\gamma$) and from fermion loops (for all) (Fig. 3.15).

We reproduce here the results for $\Gamma(H \rightarrow \gamma\gamma)$ and $\Gamma(H \rightarrow gg)$ [64, 66]:

$$\Gamma(H \rightarrow \gamma\gamma) = \frac{G_F \alpha^2 m_H^3}{128\pi^3 \sqrt{2}} |A_W(\tau_W) + \sum_f N_C Q_f^2 A_f(\tau_f)|^2 \quad (3.118)$$

$$\Gamma(H \rightarrow gg) = \frac{G_F \alpha_s^2 m_H^3}{64\pi^3 \sqrt{2}} \left| \sum_{f=Q} A_f(\tau_f) \right|^2 \quad (3.119)$$

Fig. 3.15 One-loop diagrams for Higgs decay into $\gamma\gamma$, $Z\gamma$ and gg



where $\tau_i = m_H^2/4m_i^2$ and:

$$A_f(\tau) = \frac{2}{\tau^2}[\tau + (\tau - 1)f(\tau)]$$

$$A_W(\tau) = -\frac{1}{\tau^2}[2\tau^2 + 3\tau + 3(2\tau - 1)f(\tau)] \quad (3.120)$$

with:

$$f(\tau) = \arcsin^2 \sqrt{\tau} \quad \text{for } \tau \leq 1$$

$$f(\tau) = -\frac{1}{4} \left[\log \frac{1 + \sqrt{1 - \tau^{-1}}}{1 - \sqrt{1 - \tau^{-1}}} - i\pi \right]^2 \quad \text{for } \tau > 1 \quad (3.121)$$

For $H \rightarrow \gamma\gamma$ (as well as for $H \rightarrow Z\gamma$) the W loop is the dominant contribution at small and moderate m_H . We recall that the $\gamma\gamma$ mode can be a possible channel for Higgs discovery only for m_H near its lower bound (i.e for $114 < m_H < 150$ GeV). In this domain of m_H we have $\Gamma(H \rightarrow \gamma\gamma) \sim 6\text{--}23$ KeV. For example, in the limit $m_H \ll 4m_i^2$, or $\tau \rightarrow 0$, we have $A_W(0) = -7$ and $A_f(0) = 4/3$. The two contributions become comparable only for $m_H \sim 650$ GeV where the two amplitudes, still of opposite sign, nearly cancel. The top loop is dominant among fermions (lighter fermions are suppressed by m_f^2/m_H^2 modulo logs) and, as we have seen, it approaches a constant for large m_t . Thus the fermion loop amplitude for the Higgs would be sensitive to effects from very heavy fermions, in particular the $H \rightarrow gg$ effective vertex would be sensitive to all possible very heavy coloured quarks. As discussed in the QCD Chapter (Chap. 4) the $gg \rightarrow H$ vertex provides one of the main production channels for the Higgs at hadron colliders.

3.14 Limitations of the Standard Model

No signal of new physics has been found neither in electroweak precision tests nor in flavour physics. Given the success of the SM why are we not satisfied with this theory? Why not just find the Higgs particle, for completeness, and declare that particle physics is closed? The reason is that there are both conceptual problems and phenomenological indications for physics beyond the SM. On the conceptual side the most obvious problems are that quantum gravity is not included in the SM and the related hierarchy problem. Among the main phenomenological hints for new

physics we can list coupling unification, dark matter, neutrino masses (discussed in Sect. (3.7)), baryogenesis and the cosmological vacuum energy.

The computed evolution with energy of the effective SM gauge couplings clearly points towards the unification of the electro-weak and strong forces (GUT's) at scales of energy $M_{GUT} \sim 10^{15} - 10^{16}$ GeV [31] which are close to the scale of quantum gravity, $M_{Pl} \sim 10^{19}$ GeV. One is led to imagine a unified theory of all interactions also including gravity (at present superstrings provide the best attempt at such a theory). Thus GUT's and the realm of quantum gravity set a very distant energy horizon that modern particle theory cannot ignore. Can the SM without new physics be valid up to such large energies? One can imagine that some obvious problems could be postponed to the more fundamental theory at the Planck mass. For example, the explanation of the three generations of fermions and the understanding of fermion masses and mixing angles can be postponed. But other problems must find their solution in the low energy theory. In particular, the structure of the SM could not naturally explain the relative smallness of the weak scale of mass, set by the Higgs mechanism at $\mu \sim 1/\sqrt{G_F} \sim 250$ GeV with G_F being the Fermi coupling constant. This so-called hierarchy problem is due to the instability of the SM with respect to quantum corrections. This is related to the presence of fundamental scalar fields in the theory with quadratic mass divergences and no protective extra symmetry at $\mu = 0$. For fermion masses, first, the divergences are logarithmic and, second, they are forbidden by the $SU(2) \otimes U(1)$ gauge symmetry plus the fact that at $m = 0$ an additional symmetry, i.e. chiral symmetry, is restored. Here, when talking of divergences, we are not worried of actual infinities. The theory is renormalizable and finite once the dependence on the cut off Λ is absorbed in a redefinition of masses and couplings. Rather the hierarchy problem is one of naturalness. We can look at the cut off as a parameterization of our ignorance on the new physics that will modify the theory at large energy scales. Then it is relevant to look at the dependence of physical quantities on the cut off and to demand that no unexplained enormously accurate cancellations arise.

The hierarchy problem can be put in very practical terms (the “little hierarchy problem”): loop corrections to the Higgs mass squared are quadratic in Λ . The most pressing problem is from the top loop. With $m_h^2 = m_{bare}^2 + \delta m_h^2$ the top loop gives

$$\delta m_{h|top}^2 \sim -\frac{3G_F}{2\sqrt{2}\pi^2} m_t^2 \Lambda^2 \sim -(0.2\Lambda)^2 \quad (3.122)$$

If we demand that the correction does not exceed the light Higgs mass indicated by the precision tests, Λ must be close, $\Lambda \sim o(1 TeV)$. Similar constraints arise from the quadratic Λ dependence of loops with gauge bosons and scalars, which, however, lead to less pressing bounds. So the hierarchy problem demands new physics to be very close (in particular the mechanism that quenches the top loop). Actually, this new physics must be rather special, because it must be very close, yet its effects are not clearly visible neither in precision electroweak tests (the “LEP Paradox” [67]) nor in flavour changing processes and CP violation. Examples of proposed classes of solutions for the hierarchy problem are: (1) Supersymmetry

[68]. In the limit of exact boson-fermion symmetry the quadratic divergences of bosons cancel so that only log divergences remain. However, exact SUSY is clearly unrealistic. For approximate SUSY (with soft breaking terms), which is the basis for all practical models, Λ is replaced by the splitting of SUSY multiplets, $\Lambda^2 \sim m_{SUSY}^2 - m_{ord}^2$. In particular, the top loop is quenched by partial cancellation with s-top exchange, so the s-top cannot be too heavy. (2) Technicolor [69]. The Higgs system is a condensate of new fermions. There is no fundamental scalar Higgs sector, hence no quadratic divergences associated to the μ^2 mass in the scalar potential. This mechanism needs a very strong binding force, $\Lambda_{TC} \sim 10^3 \Lambda_{QCD}$. It is difficult to arrange that such nearby strong force is not showing up in precision tests. Hence this class of models has been disfavoured by LEP, although some special class of models have been devised a posteriori, like walking TC, top-color assisted TC etc (for recent reviews, see, for example, [69]). (3) Extra dimensions (for a recent review, see, for example, [70]). The idea is that M_{Pl} appears very large, or equivalently that gravity appears very weak, because we are fooled by hidden extra dimensions so that either the real gravity scale is reduced down to a lower scale, even possibly down to $o(1 \text{ TeV})$ or the intensity of gravity is red shifted away by an exponential warping factor [71]. This possibility is very exciting in itself and it is really remarkable that it is compatible with experiment. It provides a very rich framework with many different scenarios. (4) “Little Higgs” models [72]. In these models the Higgs is a pseudo-Goldstone boson and extra symmetries allow $m_h \neq 0$ only at two-loop level, so that Λ can be as large as $o(10 \text{ TeV})$ with the Higgs within present bounds (the top loop is quenched by exchange of heavy vectorlike new quarks with charge $2/3$). The physics beyond the SM will be discussed in Chap. 8.

Acknowledgments I am very grateful to Giuseppe Degrassi, Paolo Gambino, Martin Grunewald, Vittorio Lubicz for their help and advise.

References

1. S.L. Glashow, Nucl. Phys. **22** (1961) 579; S. Weinberg, Phys. Rev. Lett. **19** (1967) 1264; A. Salam, in *Elementary Particle Theory*, ed. N. Svartholm (Almqvist and Wiksells, Stockholm, 1969), p. 367.
2. F. Englert, R. Brout, Phys.Rev.Lett.**13**, 321 (1964); P.W. Higgs, Phys.Lett. **12**,132 (1964).
3. E.D.Commins, *Weak interactions*, Mc Graw Hill, 1973; L. V. Okun, *Leptons and Quarks*, North Holland, 1982; D. Bailin, *Weak Interactions*, 2nd e., Hilger, 1982; H. M. Georgi, *Weak interactions and modern particle theory*, Benjamin, 1984.
4. J.D. Bjorken and S. Drell, *Relativistic Quantum Mechanics/Fields*, Vols. I, II, McGraw-Hill, New York, (1965).
5. Particle Data Group, The Journal of Physics G 33(2006)1.
6. G.Altarelli, T.Sjöstrand and F.Zwirner (eds.), “Physics at LEP2”, CERN Report 95-03.
7. The ALEPH, DELPHI, L3, OPAL, SLD Collaborations and the LEP Electroweak Working Group, *A Combination of Preliminary Electroweak Measurements and Constraints on the Standard Model*, hep-ex/0312023, and references therein.
8. The LEP Electroweak Working Group, <http://lepewwg.web.cern.ch/LEPEWWG/>.

9. J. Ellis, J. M. Gaillard and D. V. Nanopoulos, Nucl. Phys. B106 (1976) 292; J. D. Bjorken, SLAC Report 198 (1976).
10. G. Altarelli, B. Mele and F. Pitolli, Nucl. Phys. B287 (1987) 205.
11. G. Altarelli, T. Sjostrand and F. Zwirner, *Physics at LEP2*, CERN Report 96-01, (1996), pag. 361–366.
12. N. Cabibbo, Phys. Rev. Lett., 10 (1963) 531; M. Kobayashi and T. Maskawa, Progr. Th. Phys. 49 (1973) 652.
13. S.L. Glashow, J. Iliopoulos and L. Maiani, Phys. Rev. D2 (1970) 1285.
14. L. Maiani, *Proc. Int. Symp. on Lepton and Photon Interactions at High Energy*, Hamburg, 1977.
15. L. Wolfenstein, Phys. Rev. Lett., 51 (1983) 1945.
16. The Unitary Triangle Fit Group, <http://www.utfit.org>
17. <http://ckmfitter.in2p3.fr/>
18. C. Jarlskog, Phys. Rev. Lett., 55 (1985) 1039.
19. J. F. Donoghue, E. Golowich and B. Holstein, *Dynamics of the standard model*, Cambridge Univ. Press, 1992.
20. T. Becher and M. Neubert, Phys.Rev.Lett.98:022003,2007, [hep-ph 0610067]; see also M. Misiak et al, Phys.Rev.Lett.98:022002,2007 [hep-ph/0609232].
21. G.L. Fogli et al, *Proceedings of the 40th Rencontres de Moriond on Electroweak Interactions and Unified Theories*, La Thuile, Italy, hep-ph/0506307; M. Maltoni et al, New J. Phys. 6 (2004) 122, [hep-ph/0405172].
22. K. Zuber, Acta Phys.Polon.B37:1905–1921,2006; [nucl-ex/0610007].
23. J. Lesgourgues and S. Pastor, Phys.Rept.429:307–379,2006; [astro-ph/0603494].
24. P. Minkowski, Phys. Lett. B67 (1977) 421; T. Yanagida, in *Proc. of the Workshop on Unified Theory and Baryon Number in the Universe*, KEK (1979); S. L. Glashow, in *Quarks and Leptons*, Cargèse, ed. M. Lévy et al., Plenum (1980); M. Gell-Mann, P. Ramond and R. Slansky, in *Supergravity*, Stony Brook (1979); R. N. Mohapatra and G. Senjanovic, Phys. Rev. Lett., 44 (1980) 912.
25. Ta-Pei Cheng and Ling-Fong Li, *Gauge theory of elementary particle physics*, Oxford Univ. Press, (1988); D. Bailin and A. Love, *Introduction to gauge field theory (Revised edition)*, (1993); D. Y. Bardin and G. Passarino, *The standard model in the making : precision study of the electroweak interactions*; Oxford Clarendon Press, (1999).
26. J.M. Cornwall, D.N. Levin and G. Tiktopoulos, Phys. Rev. D10, 1145 (1974); C.E. Vayonakis, Lett. Nuovo Cim. 17, 383 (1976); B.W. Lee, C. Quigg and H. Thacker, Phys. Rev. D16, 1519 (1977); M. S. Chanowitz and M. K. Gaillard, Nucl. Phys. B261, 379 (1985).
27. M. Veltman, Nucl. Phys. B21, 288 (1970); G.'t Hooft, Nucl. Phys. B33, 173 (1971); B35, 167 (1971).
28. B.W. Lee and J. Zinn-Justin, Phys. Rev. D5, 3121; 3137 (1972); D7, 1049 (1973).
29. C. Bouchiat, J. Iliopoulos and P. Meyer, Phys.Lett.B38:519,1972.
30. S. L. Adler, Phys.Rev.177:2426,1969; S. L. Adler and W. A. Bardeen, Phys.Rev.182:1517,1969; J.S. Bell and R. Jackiw, Nuovo Cim. A60:47,1969; W. A. Bardeen, Phys. Rev. 184 (1969) 1848.
31. G.G.Ross, “Grand Unified Theories”, Benjamin, 1985; R.N.Mohapatra, “Unification and Supersymmetry” Springer-Verlag, 1986; S. Raby, hep-ph/0608183. [32] G. 't Hooft, Phys.Rev.Lett.37:8,1976; Phys. Rev. D 14 (1976) 3432 [Erratum-ibid. D 18 (1978) 2199].
32. G. 't Hooft, Phys.Rev.Lett.37:8,1976.
33. A. Belavin, A. Polyakov, A. Shvarts and Y. Tyupkin, Phys. Lett. B 59 (1975) 85.
34. W. Buchmuller, R.D. Peccei and T. Yanagida, Ann.Rev.Nucl.Part.Sci.55:311,2005; [hep-ph 0502169].
35. B. Odom, D. Hanneke, B. D'Urso and G. Gabrielse, Phys. Rev. Lett. 97: 030801 (2006).
36. Muon g-2 Collab., G. W. Bennett et al, Phys. Rev. D73, 072003 (2006).
37. G. Gabrielse et al, Phys.Rev.Lett. 97:030802,2006.

38. T. Kinoshita and N. Nio, *Phys. Rev. D* **73**, 013003(2006).
39. T. Aoyama, M. Hayakawa, T. Kinoshita and M. Nio, *Phys. Rev. Lett.* **99** (2007) 110406 [arXiv:0706.3496 [hep-ph]]. T. Aoyama, M. Hayakawa, T. Kinoshita and N. Nio, hep-ph/0706.3496.
40. M. Passera, *Nucl. Phys. Proc. Suppl.* **169** (2007) 213 [hep-ph/0702027 [HEP-PH]].
41. M. Davier, *Nucl. Phys. Proc. Suppl.* **169** (2007) 288 [hep-ph/0701163].
42. G. Altarelli, R. Kleiss and C. Verzegnassi (eds.), *Z Physics at LEP1 (CERN 89- 08, Geneva, 1989)*, Vols. 1–3; Precision Calculations for the Z Resonance, ed. by D. Bardin, W. Hollik and G. Passarino, CERN Rep 95-03 (1995); M.I. Vysotskii, V.A. Novikov, L.B. Okun and A.N. Rozanov, hep-ph/9606253 or *Phys.Usp.*39:503–538,1996.
43. T. Appelquist and J. Carazzone, *Phys.Rev.D*11:2856,1975.
44. J. van der Bij and M.J.G. Veltman, *Nucl.Phys.B*231:205,1984.
45. The LEP and SLD Collaborations, *Phys. Rep.* **427** (2006) 257, hep-ex/0509008.
46. M. Awramik and M. Czakon, *Phys. Rev. Lett.* **89** (2002) 241801, [hep-ph/0208113]. M. Awramik, M. Czakon, A. Onishchenko and O. Veretin, *Phys. Rev. D* **68** (2003) 053004, [hep-ph/0209084]. M. Awramik and M. Czakon, *Phys. Lett. B* **568** (2003) 48, [hep-ph/0305248]. A. Freitas, W. Hollik, W. Walter and G. Weiglein, *Phys. Lett. B* **495** (2000) 338, [Erratum-ibid. B **570** (2003) 260], [hep-ph/0007091]. A. Freitas, W. Hollik, W. Walter and G. Weiglein, *Nucl. Phys. B* **632** (2002) 189, [Erratum-ibid. B **666** (2003) 305], [hep-ph/0202131]. A. Onishchenko and O. Veretin, *Phys. Lett. B* **551** (2003) 111 [hep-ph/0209010].
47. K. G. Chetyrkin, M. Faisst, J. H. Kuhn, P. Maierhofer and C. Sturm, *Phys. Rev. Lett.* **97** (2006) 102003, hep-ph/0605201; R. Boughezal and M. Czakon, *Nucl. Phys. B* **755** (2006) 221, [hep-ph/0606232].
48. M. Awramik, M. Czakon, A. Freitas and G. Weiglein, *Phys. Rev. Lett.* **93** (2004) 201805, [hep-ph/0407317]; M. Awramik, M. Czakon and A. Freitas, hep-ph/0608099; *Phys. Lett. B* **642** (2006) 563, [hep-ph/0605339]; W. Hollik, U. Meier and S. Uccirati, hep-ph/0610312.
49. G. Altarelli, R. Barbieri and F. Caravaglios, *Int. J. Mod. Phys. A* 13(1998)1031 and references therein.
50. M.E. Peskin and T. Takeuchi, *Phys. Rev. Lett.* **65** (1990) 964; *Phys. Rev. D*46 (1991) 381.
51. See, for example, M. Lindner, *Z. Phys.* **31**, 295 (1986); T. Hambye and K. Riesselmann, *Phys. Rev. D***55**, 7255 (1997); hep-ph/9610272.
52. The NuTeV Collaboration, G.P. Zeller et al., *Phys. Rev. Lett.* **88** (2002) 091802.
53. M. Yu. Kuchiev and V. V. Flambaum, hep-ph/0305053.
54. The SLAC E158 Collaboration, P.L. Anthony et al., hep-ex/0312035, hep-ex/0403010.
55. P. Gambino, *Int.J.Mod.Phys.A*19:808,2004, [hep-ph/0311257].
56. D. Choudhury, T.M.P. Tait and C.E.M. Wagner, *Phys. Rev. D* **65** (2002) 053002, hep-ph/0109097.
57. A. Djouadi, G. Moreau and F. Richard, *Nucl. Phys. B* **773** (2007) 43 [hep-ph/0610173].
58. N. Cabibbo, L. Maiani, G. Parisi and R. Petronzio, *Nucl. Phys.* **B158**,295 (1979).
59. M. Sher, *Phys. Rep.* **179**, 273 (1989); *Phys. Lett.* **B317**, 159 (1993).
60. G. Altarelli and G. Isidori, *Phys. Lett.* **B337**, 141 (1994); J.A. Casas, J.R. Espinosa and M. Quirós, *Phys. Lett.* **B342**, 171 (1995); J.A. Casas et al., *Nucl. Phys.* **B436**, 3 (1995); **EB439**, 466 (1995); M. Carena and C.E.M. Wagner, *Nucl. Phys.* **B452**, 45 (1995).
61. G. Isidori, G. Ridolfi and A. Strumia; *Nucl. Phys.* **B609**,387 (2001).
62. T. Hambye and K. Riesselmann, *Phys.Rev.D*55:7255,1997.
63. B. W. Lee, C. Quigg and H.B. Thacker, *Phys.Rev. D*16:1519,1977.
64. A. Djouadi, hep-ph/0503172.
65. E. Accomando et al., *Phys. Rep.* 299 (1998) 1.
66. H. E. Haber, G. Kane, S. Dawson and J. F. Gunion, *The Higgs Hunter's Guide*, Westview, 1990.
67. R. Barbieri and A. Strumia, hep-ph/0007265.
68. H.P. Nilles, *Phys. Rep.* C110 (1984) 1; H.E. Haber and G.L. Kane, *Phys. Rep.* C117 (1985) 75; R. Barbieri, *Riv. Nuovo Cim.* 11 (1988) 1; S. P. Martin, hep-ph/9709356; M. Drees, R. Godbole and P. Roy, *Theory and Phenomenology of Sparticles*, World Sci. (2004).
69. K. Lane, hep-ph/0202255; R.S. Chivukula, hep-ph/0011264.

70. R. Rattazzi, hep-ph/ 0607055.
71. L. Randall and R. Sundrum, Phys. Rev. Lett. 83 (1999) 3370; 83 (1999) 4690. W.D. Goldberger and M. B. Wise, Phys. Rev. Letters 83 (1999) 4922.
72. M. Schmaltz, hep-ph/0210415; H. C. Cheng and I. Low, JHEP **0408** (2004) 061 [hep-ph/0405243]; J. Hubisz, P. Meade, A. Noble and M. Perelstein, JHEP **0601** (2006) 135 [hep-ph/0506042].

Open Access This chapter is licensed under the terms of the Creative Commons Attribution 4.0 International License (<http://creativecommons.org/licenses/by/4.0/>), which permits use, sharing, adaptation, distribution and reproduction in any medium or format, as long as you give appropriate credit to the original author(s) and the source, provide a link to the Creative Commons licence and indicate if changes were made.

The images or other third party material in this chapter are included in the chapter's Creative Commons licence, unless indicated otherwise in a credit line to the material. If material is not included in the chapter's Creative Commons licence and your intended use is not permitted by statutory regulation or exceeds the permitted use, you will need to obtain permission directly from the copyright holder.

